EXPERIMENTAL DETERMINATION OF KINETIC FRACTIONATION OF CARBON AND OXYGEN ISOTOPES DURING CO_2 HYDRATION

A THESIS SUBMITTED TO THE GRADUATE DIVISION OF THE UNIVERSITY OF HAWAI'I AT MĀNOA IN PARTIAL FULFILLMENT OF THE REQUIREMENTS FOR THE DEGREE OF

MASTER OF SCIENCE

IN

OCEANOGRAPHY

AUGUST 2019

By

Lauren Michele Yumol

Thesis Committee:

Richard Zeebe, Chairperson
Michael Guidry
Brian Popp

ACKNOWLEDGEMENT

I would like to give my utmost thanks to my thesis advisor Richard Zeebe and my co-advisor Joji Uchikawa for not only providing me with the opportunity to work on this project, but also for their encouragement, patience, and knowledge over the last few years which has helped shape my scientific experience. I also appreciate the thoughtful advice both Richard and Joji provided me which gave me the motivation needed to persevere through any difficulties I encountered. I would like to thank my committee members, Michael Guidry and Brian Popp, for their insight and wisdom. Thank you to Dustin Harper and Colin Carney at the Stable Isotope Lab at UCSC for analyzing my carbonate samples and for always providing a fast turnaround on results.

A special thanks to the Marine Geology and Geochemistry Division faculty for all of the help provided both in the lab and in the classroom. I would like to thank Van Tran for her hard work and dedication to her job, which aided my success as a graduate student. Thank you to the entire oceanography faculty and staff for providing a supportive work environment. I am grateful that Richard Zeebe and Joji Uchikawa were awarded the funding for this project by NSF and thankful that NSF approved their proposal, I would not be here if it weren't for my advisor and co-advisor who work hard to secure the funding for this project.

Finally, I would like to thank Jasper, my mom, dad, brother and my family and friends, who supported me throughout my entire college education and especially supportive during my graduate school career. I am so lucky to have had support I received from these special people over the years.

ABSTRACT

The CO_2 hydration reaction is a fundamental chemical transformation involved in various physicochemical, geochemical, and biological processes, and essential in aqueous solutions that contain dissolved inorganic carbon (DIC). In marine environments, the CO_2 hydration reaction and its affiliated products (i.e. H_2CO_3, HCO_3^-, CO_3^{2-}, and H^+) play a critical role in regulating ocean pH, biogenic and inorganic mineral precipitation, biological carbon fixation, carbon sequestration, and more. There is a characteristic kinetic isotope effect (KIE) that is associated with the CO_2 hydration reaction, which causes the reaction product to be depleted in the heavy isotopes of carbon and oxygen. It is important to understand how KIEs influence carbon and oxygen isotope compositions because the isotopic compositions of substances or compounds that form from HCO_3^- (i.e. the product of CO_2 hydration ($CO_2 + H_2O$)), for example carbonate minerals used as indicators of past environments, will also be affected. Despite evidence of KIEs occurring in the environment, there are only a few experimental studies that have attempted to characterize kinetic isotope fractionation (KIF) during the hydration of CO_2, but the KIFs reported in those studies suggest more experimental work is needed to better define KIEs during CO_2 hydration. In Chapter 1, we define important terminology that will be used throughout this thesis, describe the KIEs that are associated with the CO_2 hydration reaction, and explain how KIF is related to equilibrium isotope fractionation. We will also discuss the previous experimental and theoretical studies and the KIFs reported in those studies. The overall purpose and main objective of this study is to produce the most reliable experimental data available today by experimentally determining KIEs during CO_2 hydration in carbon and oxygen isotopes.

TABLE OF CONTENTS

LIST OF FIGURES

(purple arrows; *i.e. 2‰ less than if compared to $CO_{2\,(g)}$ (magenta arrows; Mook, 1986)), where $CO_{2\,(g)}$ of Batch-4 was derived from Eq. (2.7) and the measured $\delta^{13}C$ value of $NaHCO_3$, and the $CO_{2\,(g)}$ from McConnaughey was directly measured. The ^{13}KIF between $CO_{2\,(g)}$ and $CO_{2\,(aq)}$ (Eq. (2.17)) and the $\delta^{13}C$ values for $CO_{2\,(g)}$ from Batch-4 and McConnaughey were used to calculate the final ^{13}KIF between $BaCO_3$/ $CaCO_3$ and $CO_{2\,(aq)}$. **B)** The ^{18}KIFs of Batch-4 (left of axis) and McConnaughey (1989) (right of axis). The line labelled δ_{CaCO_3} on the right side of the center axis represents the $\delta^{18}O$ value of $CO_{2\,(g)}$ liberated from $CaCO_3$ by acid dissolution in equilibrium with VSMOW. **The acid fractionation factor between the liberated $CO_{2\,(g)}$ and the solid $CaCO_3$ is ~10.2‰, so the true $\delta^{18}O$ value of McConnaughey's solid $CaCO_3$ is ~10.2‰ lighter than δ_{CaCO_3} (black arrow), which will be the value used to calculate ^{18}KIFs that can be directly compared to ^{18}KIFs of Batch-4. The ^{18}KIF between $BaCO_3$ and $CO_{2\,(g)}$ (magenta arrow) was determined from the $\delta^{18}O$ value of $CO_{2\,(g)}$ derived from the relationship between Eq. (2.10) ($^{18}\varepsilon_{CO_{2\,(g)}-H_2O}$; light blue arrow) and the measured $\delta^{18}O$ value of H_2O (-3.1‰). The same ^{18}KIF for McConnaughey was calculated using the measured $\delta^{18}O$ value of $CO_{2\,(g)}$ used in the experiments. The ^{18}KIF we defined from Eq. (2.12) is given by the green arrow

Fig. 2.6. A comparison between ^{13}KIFs and ^{18}KIFs of Batch-4 between $CO_{2\,(g)}$ and $BaCO_3$ at T = 18°C (green triangles) and 25°C (red circles), and the ^{13}KIFs and ^{18}KIFs between $CO_{2\,(g)}$ and $CaCO_3$ reported by McConnaughey (1989) at T = 21°C (dark blue circles) and 1.1 to 4.3°C (light blue circles). The positive increase in ^{13}KIFs and ^{18}KIFs indicates stronger ^{13}C and ^{18}O depletions in $BaCO_3$ (or $CaCO_3$) relative to equilibrium $CO_{2\,(g)}$

LIST OF TABLES

LIST OF EQUATIONS

CHAPTER 1 EQUATIONS

CHAPTER 2 EQUATIONS

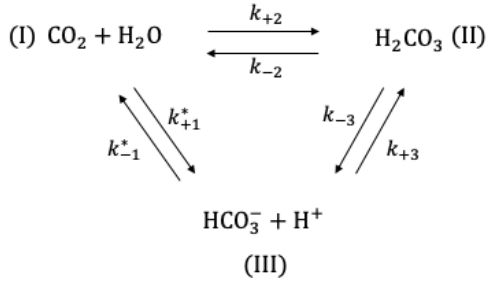

CHAPTER 1. INTRODUCTION

1.1 The CO_2 Hydration Reaction

The hydration of carbon dioxide (CO_2) in marine and aqueous environments is a key reaction involved in several physicochemical, geochemical, and biochemical systems. Specifically, the CO_2 hydration reaction is known for the essential role it plays in major oceanic processes such as ocean acidification, biological and inorganic mineral precipitation, carbon fixation, CO_2 sequestration, etc. (Caldeira and Wickett, 2003; Dunsmore, 1992; Brown et al., 2009; Hopkinson et al., 2011; Stirling, 2011; Tresguerres and Hamilton, 2017). A kinetic isotope effect (KIE) is associated with this reaction, where the reaction product is typically depleted in the heavy isotopes of carbon (^{13}C) and oxygen (^{18}O) relative to the reactant (Bigeleisen and Wolfsberg, 1958; Zeebe & Wolf-Gladrow, 2001). These KIEs are expressed in chemical reactions when reaction rates (k) of a compound containing the heavy and light isotope differ (Hayes, 2001). For example, the reaction for the CO_2 hydration can be independently written in two forms for ^{12}C and ^{13}C isotopes:

$$^{12}CO_2 + H_2O \underset{^{12}k_-}{\overset{^{12}k_+}{\rightleftharpoons}} H^{12}CO_3^- + H^+ \quad (1.1a)$$

$$^{13}CO_2 + H_2O \underset{^{13}k_-}{\overset{^{13}k_+}{\rightleftharpoons}} H^{13}CO_3^- + H^+ \quad (1.1b)$$

Because the reaction rate constant for CO_2 hydration involving $^{12}CO_2$ ($^{12}k_+$) is greater than the other counterpart for $^{13}CO_2$ ($^{13}k_+$), the reaction product HCO_3^- will be depleted in ^{13}C with respect to the $CO_{2(aq)}$ as a result of KIE for the CO_2 hydration reaction, which is given by $^{12}k_+/^{13}k_+$ (also note that KIE for the reverse reaction, or HCO_3^- dehydration is given by

$^{12}k_-/^{13}k_-$). Furthermore, KIE and the equilibrium fractionation (α) for the same chemical reaction is related by:

$$\frac{^{13}K'}{^{12}K} = \alpha = \left(\frac{^{13}k'_+}{^{13}k'_-}\right)\left(\frac{^{12}k_-}{^{12}k_+}\right) \quad (1.2)$$

where K and K' are equilibrium constants for the reactions of ^{12}C and ^{13}C, respectively (Eq. (1.1a) and (1.1b); Zeebe and Wolf-Gladrow, 2001). Also note that the reactions (Eq. (1.1a) and (1.1b)) as well as the definition of KIE illustrated above can be analogously written for oxygen isotopes ^{16}O and ^{18}O, where KIE for CO_2 hydration is given by $^{16}k_+/^{18}k_+$. From this point forward, KIE in terms of carbon and oxygen isotopes is denoted as ^{13}KIE and ^{18}KIE, respectively.

Apparent ^{13}C and ^{18}O depletions relative to the expected thermodynamic equilibrium have been observed for both natural and laboratory grown carbonate minerals (e.g. Coplen et al., (1994), Daëron et al. (2019), Kim and O'Neil (2007), and Watkins et al., (2013)), which are to some extent attributed to KIEs associated with CO_2 hydration. Yet, to date, KIEs for CO_2 hydration are not well constrained in terms of both carbon and oxygen isotopes, which is exemplified by the inconsistencies in the proposed magnitude of KIEs in previous experimental and theoretical studies (Marlier and O'Leary, 1984; Clark and Lauriol, 1992; Guo, 2008; Zeebe, 2014; Sade and Halevy, 2017).

This study aims to experimentally constrain kinetic isotope fractionation factors (KIF; i.e. ^{13}KIF and ^{18}KIF for carbon and oxygen, respectively) during CO_2 hydration. The experimental setup used in this study was adapted from McConnaughey (1989) but with important modifications, which will be discussed in more details in Chapter 2. The results from our

precipitation experiments will help define the magnitude of KIFs during CO_2 hydration and provide the experimental data necessary to evaluate the accuracy of theoretical calculations.

1.2 Previous Studies

There are only a few studies that attempted to determine KIEs during CO_2 hydration/ HCO_3^- dehydration. Clark and Lauriol (1992) experimentally grew cryogenic calcite and determined ^{13}KIF and ^{18}KIF associated with HCO_3^- dehydration to be ~ 32.0‰ and ~ 6‰, respectively, at 0°C. Provided with the carbon and oxygen α (Zhang et al., 1995 and Beck et al., 2005) and the KIEs for HCO_3^- dehydration determined by Clark and Lauriol, ^{13}KIE and ^{18}KIE during CO_2 hydration can be calculated as 19.7‰ and 3.7‰, respectively, based on the relationship given by Eq. (1.2) (Zeebe, 2014; Sade and Halevy, 2017). However, the mineralogical formation of cryogenic calcite is uncertain, so the KIEs Clark and Lauriol originally calculated may not be characteristic of calcite but rather another type of polymorph such as vaterite or ikaite (Lacella et al., 2009; Sade and Halevy, 2017). In another experimental study, Marlier and O'Leary (1984) developed methods to determine ^{13}KIEs during CO_2 hydration and HCO_3^- dehydration. For CO_2 hydration, phosphoenolpyruvate (PEP) carboxylase was used to catalyze rapid precipitation of HCO_3^- to form malate. For HCO_3^- dehydration, CO_2 degassed from buffered $NaHCO_3$ solution by helium sweeping was trapped using liquid nitrogen. Based on subsequent isotope analyses on the resultant malate and CO_2 gas, they reported a ^{13}KIF during CO_2 hydration of ~6.9‰ at 24°C. However, in a subsequent study performed by the same group (O'Leary et al., 1992), the ^{13}KIF is oddly reported as 13‰, not 6.9‰ with no further explanation.

Theoretical calculations have also been employed to quantify KIEs associated with CO_2 hydration. Guo (2008) theoretically calculated the ^{18}KIF during HCO_3^- dehydration and reported an ^{18}O depletion in CO_2 relative to HCO_3^- of ~7‰ at 25°C. Sade and Halevy (2017;2018) reported a ^{18}KIF during CO_2 hydration of ~16.4‰ using the relationship between ^{18}KIF for HCO_3^- dehydration reported by Guo (2008) and $^{18}\alpha$ from Beck et al. (2005). However, a more recent theoretical study by Guo and Zhou (2019) reported an estimated ^{18}KIF for the hydration of CO_2 of 4.3‰ at 25°C. Zeebe (2014) reported ^{13}KIF and ^{18}KIF at 25°C to be between ~ 23 and 33‰ and ~13 and 15‰, respectively. These values were based on theoretical calculations where it was assumed that the hydration of CO_2 proceeds in a stepwise fashion through a $HCO_3^- - H_3O^+$ intermediate state rather than directly to the product (H_2CO_3), with each pathway leading to different KIFs (for review, see Section 2 in Chapter 2 or Zeebe, 2014). However, whether or not the CO_2 hydration reaction follows a direct or stepwise pathway is still uncertain. The ^{18}KIFs by Zeebe (2014) reported were calculated using H_2CO_3 as the product of CO_2 hydration and compared the isotopic rate constants for CO_2 hydration to the fractionation between instantaneously produced H_2CO_3 and CO_2 in isotopic equilibrium with H_2O. However, Sade and Halevy (2017; 2018) separated the individual components of the equilibrium fractionation factor (i.e. CO_2 and H_2O) to calculate the ^{18}KIF between HCO_3^- relative to CO_2 and H_2O as two separate ^{18}KIFs. The revised ^{18}KIFs reported by Sade and Halevy for HCO_3^- relative to CO_2 and HCO_3^- relative to H_2O is between 4.3 and 6.2‰ and 0 to 9.6‰, respectively. McConnaughey (1989) conducted calcite precipitation experiments in an attempt to replicate kinetic isotope disequilibrium observed in biogenic carbonates. Although his experimental data at 21°C show ^{18}O and ^{13}C depletions of ~5‰ and ~8.3‰, respectively, relative to $\delta^{13}C$ and $\delta^{18}O$ values estimated for CO_2 in isotopic equilibrium with Galapagos seawater, we have concerns for the

values derived from McConnaughey's precipitation experiments. First, there was no control on solution pH, such that it varied between pH 7.4 and 8.5 during $CaCO_3$ precipitation. Controlling the solution pH is critical because it dictates whether CO_2 hydration (predominant at low pH) or CO_2 hydroxylation (predominant at high pH) is the primary reaction during precipitation (see Section 2 in Chapter 2 for details). Thus, there is a chance that McConnaughey's (1989) experimental carbonates do not fully record the KIE associated with CO_2 hydration. Second, the ^{13}C and ^{18}O depletions of McConnaughey's experimental $CaCO_3$ were scaled relative to the $\delta^{13}C$ and $\delta^{18}O$ value of the CO_2 source gas. However, the actual $\delta^{13}C$ and $\delta^{18}O$ values of the CO_2 source gas were never provided, which makes it difficult to determine the ^{13}C and ^{18}O partitioning specific to the $CO_{2(g)}$-DIC- H_2O system in his study. More details about McConnaughey (1989) will be discussed further in a later section.

In summary, the currently available experimental data is limited to a few studies and carbon and oxygen KIFs reported in the current literature are inconsistent between experimental and theoretical studies (Table 1.1). The scarcity of available data and notably large inconsistency therein (e.g. by a factor of ~5; see Table 1.1) suggest more experimental work is required in order to determine the KIE and fully understand the CO_2 hydration/dehydration mechanism.

Table 1.1. The average ^{13}KIFs and ^{18}KIFs of CO_2 hydration reported from previous experimental and theoretical studies.

Reference	T (°C)	(E)xperimental/(T)heoretical	$^{13}KIF_{CO_2-HCO_3^-}$ (‰)	$^{18}KIF_{CO_2-HCO_3^-}$ (‰)
Clark & Lauriol (1992)	0	E	19.7	3.7*
Marlier & O'Leary (1984)	24	E	6.9	--
O'Leary et al. (1992)	24	E	13	--
McConnaughey (1989)	21	E	8.3	5
Zeebe (2014)	25	T	23-33 ($n \geq 4$)	13-15 ($n \geq 4$)[a]
Zeebe (2014)			10-14($n \leq 3$)	10.5-15 ($n \leq 3$)
	25	T	--	5.2*
Guo (2008)	0	T	--	16.4
Guo & Zhou (2019)	25	T		4.3

*The values reevaluated by Sade and Halevy (2017 and 2018).
[a]KIF between $CO_{2(g)}$ and H_2CO_3

1.3 Delta Notation & Isotope Fractionation Factors

In stable isotope geochemistry, isotopic abundances are measured in a material or sample and can be used as a tool to reveal underlying mechanisms involved in the formation of the material. Isotopic abundances are reported as the relative difference between the isotope ratio of a sample (R_s) and an isotopically known reference standard (R_{std}) (Urey, 1948; McKinney et al., 1950; Hayes, 2002). The isotope ratios of carbon (^{13}R) and oxygen (^{18}R) are defined as the ratio of the less abundant isotope (i.e. the isotopically heavier isotope for carbon (^{13}C) and oxygen (^{18}O)), to the more abundant isotope, ^{12}C and ^{16}O:

$$^{13}R = {}^{13}\mathrm{C}/{}_{12}\mathrm{C}$$

and

$$^{18}R = {}^{18}\mathrm{O}/{}_{16}\mathrm{O}$$

Isotopic abundances yield isotopic compositions of a sample(s) and are reported using the δ notation. In terms of the isotopic composition of carbon in a sample, the notation is as follows:

$$\delta^{13}C_s = \left(\frac{^{13}R_s - ^{13}R_{std}}{^{13}R_{std}}\right) \times 1000 \quad (1.3)$$

where $\delta^{13}C_s$ is the carbon isotope composition expressed in parts per thousand (‰) of a sample relative to the same element in a reference standard (Hayes, 2001). Carbon and oxygen isotope ratios in carbonate minerals are reported relative to the reference standard 'Vienna Pee Dee Belemnite' (VPDB). Oxygen stable isotopes measured in carbonate minerals relative to the VPDB scale can be converted to a δ-value on the 'Vienna Standard Mean Ocean Water' (VSMOW) scale when necessary for calculating oxygen isotope fractionation.

Offsets or variations in isotopic compositions between compounds in the same reaction sequence can arise through physical, chemical, or biological processes, resulting in isotopic fractionation. Isotope fractionation can be quantified by the equation used calculate an isotopic fractionation factor:

$$^{A}\alpha_{a\text{-}b} = \frac{^{A}R_a}{^{A}R_b} = \frac{1000 + \delta^{A}X_a}{1000 + \delta^{A}X_b} \quad (1.4)$$

where A is the mass number of element X, and a and b are the two different phases of the reaction. An isotope fractionation factor can also be expressed in ‰:

$$^{A}\varepsilon_{a\text{-}b} = (^{A}\alpha_{a\text{-}b} - 1) \times 10^3 \approx 10^3 \times \ln(^{A}\alpha_{a\text{-}b}) \quad (1.5)$$

Isotopic fractionation is observed when a chemical phase preferentially incorporates the heavy or light isotope relative to another phase in the same reaction (Hayes, 2002; Sharp, 2007). An isotope effect refers to the physical phenomenon that occurs in certain chemical reactions and

is observed as an isotope fractionation (Zeebe and Wolf-Gladrow, 2001; Hayes, 2002). These isotope effects can occur in chemical reactions that are in thermodynamic equilibrium or in kinetically driven unidirectional reactions, the difference between the two are further discussed below.

Equilibrium isotope effects are associated with chemical reactions that are in thermodynamic equilibrium. Isotope fractionation that occurs in equilibrium reactions is caused by differences in the vibrational frequencies of different compounds containing a common element. The compound containing the heavier isotope (and thus a higher mass) will have a lower vibrational frequency and a lower zero-point energy, than the same compound containing the lighter isotope. The difference in zero-point energies with compounds containing either a heavy or light isotope is what leads to isotope fractionation. Thus, different compounds in a chemical reaction containing a common element may have different isotope ratios specific to the compound (Zeebe and Wolf-Gladrow, 2001). As a rule of thumb for equilibrium isotope effects, Bigeleisen (1965) stated "the heavy isotope goes preferentially to the chemical compound in which the element is bound most strongly". For example, the exchange of ^{12}C and ^{13}C in the equilibrium reaction between CO_2 and HCO_3^-:

$$^{12}CO_2 + H^{13}CO_3^- \rightleftharpoons {}^{13}CO_2 + H^{12}CO_3^- \quad (1.6)$$

In this reaction, ^{13}C is bound more strongly to HCO_3^- and thus, will have a $\delta^{13}C$ value that is enriched in ^{13}C relative to CO_2. Furthermore, the preferential partitioning of ^{13}C in HCO_3^- suggests that the difference in zero-point energies between $H^{12}CO_3^-$ and $H^{13}CO_3^-$ is greater than the difference between $^{12}CO_2$ and $^{13}CO_2$.

In contrast to equilibrium isotope effects, a kinetic isotope effect is associated with reactions that are incomplete and unidirectional. As described in Section 1.1, KIEs occur when reaction rates of a reaction involving the heavy or light isotope differ. The KIE associated with the hydration of CO_2 is an example of a normal KIE which occurs when the molecular compound containing the lighter isotope reacts more rapidly than the heavier isotope resulting in an accumulation of the light isotope in the product (Zeebe and Wolf-Gladrow, 2001). Because the reaction rate of the isotope with the smaller mass is faster than that of the isotope with the larger mass, the isotope ratio of the product will be depleted in the heavy isotope relative to the isotope ratio of the reactant.

In summary, equilibrium isotope effects lead to an observable fractionation between different chemical phases that are in thermodynamic equilibrium. Most equilibrium isotope fractionation factors (denoted here as either α or ε) involving the CO_2 hydration reaction are well constrained for carbon and oxygen from earlier theoretical and experimental studies (Vogel et al., 1970; Mook et al., 1986; Zhang et al., 1995; Brenninkmeijer et al., 1983; Beck et al., 2005). Calculating the values for ε between different phases of the CO_2 hydration reaction will play a critical role in this study when calculating final KIFs and will be described with more detail in a later section. Although KIF is important as well, there is a large gap between α and KIF because only a few studies have determined KIEs during CO_2 hydration, as described in Section 1.1.

In this study, we conducted laboratory experiments to constrain kinetic isotope fractionation factors (KIF; i.e. ^{13}KIF and ^{18}KIF for carbon and oxygen, respectively) during CO_2 hydration. The experimental setup used in this study was adapted from McConnaughey (1989) but with important modifications that will be discussed in detail in Chapter 2, Section 5. The results from our precipitation experiments will help define the magnitude of KIFs during

CO_2 hydration and provide the experimental data necessary to evaluate the accuracy of theoretical calculations. Final conclusions of the results of this study and future outlook is described in Chapter 3.

CHAPTER 2. EXPERIMENTAL DETERMINATION OF KINETIC FRACTIONATION OF CARBON AND OXYGEN ISOTOPES DURING CO_2 HYDRATION

ABSTRACT

Kinetic isotope effects (KIE) during the inorganic hydration of carbon dioxide (CO_2) in aqueous solution is a topic of growing interest as this phenomenon is key to several important physicochemical, geochemical, and biological processes. Despite the growing evidence of KIEs occurring in nature (e.g. speleothem calcites, skeletal formation of corals, formation of cryogenic carbonates, and more) the currently available experimental data is limited to only a few studies. In this study, we conducted laboratory experiments to constrain kinetic isotope fractionation factors during the hydration of CO_2. The experimental approach was adapted from an earlier study but with important modifications to systematically determine the kinetic isotope fractionation (KIF) of carbon and oxygen during CO_2 hydration. The setup consisted of a $NaHCO_3$ stock solution, a reactor chamber where $BaCO_3$ was rapidly precipitated from a dissolved barium chloride $BaCl_2$ + buffer solution, and a diaphragm pump to circulate internal gas throughout the system. $BaCO_3$ samples were analyzed for carbon and oxygen isotopes by isotope ratio mass spectrometer (IRMS). Results of the stable carbon and oxygen isotope analyses were separated into four batches, which were organized based on the group of samples that were analyzed in the same queue of the IRMS. We discuss possible experimental errors among the four batches and determine that our best results are from Batch-4. The average $\delta^{13}C$ and $\delta^{18}O$ values of Batch-4 $BaCO_3$ samples produced at pH 8.0 are -29.7 ± 0.10‰ (vs. VPDB) and 18.9 ± 0.20‰ (vs. VSMOW), respectively. Equilibrium $\delta^{13}C$ and $\delta^{18}O$ values of $CO_{2\,(g)}$ and instantaneously formed HCO_3^- were calculated from known equilibrium isotope fractionation factors, and used to calculate the carbon and oxygen KIFs (^{13}KIF and ^{18}KIF, respectively)

relative to Batch-4. A ^{13}KIF between $CO_{2\,(g)}$ and $CO_{2\,(aq)}$ of ~2.0‰ was determined experimentally by a previous study and if full KIF between $CO_{2\,(g)}$ and $CO_{2\,(aq)}$ is assumed then the mean Batch-4 ^{13}KIF is ~17.6 ± 0.43‰. Our final mean ^{13}KIF and ^{18}KIF are 17.6 ± 0.43‰ and 5.3± 0.09‰, respectively. These results are compared with reported KIFs of previous experimental studies and are the largest values out of all but one study, which may suggest our values are closest to full isotope disequilibrium during the hydration of CO_2.

1. INTRODUCTION

The hydration of carbon dioxide is a fundamental chemical transformation involved in several physicochemical, geochemical, and biochemical systems. In marine environments, the CO_2 hydration reaction and its affiliated ionic compounds (e.g. CO_3^{2-}, H_2CO_3, HCO_3^-, H^+) play an essential role in major oceanic processes such as, ocean acidification, biological and inorganic mineral precipitation, carbon fixation, CO_2 sequestration, etc. (Caldeira and Wickett, 2003; Dunsmore, 1992; Brown et al., 2009; Hopkinson et al., 2011; Stirling, 2011; Tresguerres and Hamilton, 2017). When the CO_2 hydration reaction proceeds unidirectionally it is associated with a kinetic isotope effect (KIE), where the reaction product is typically depleted in the heavy isotopes of carbon (^{13}C) and oxygen (^{18}O) relative to the reactant (Eq. (2.1) and (2.2); Bigeleisen and Wolfsberg, 1958; Zeebe & Wolf-Gladrow, 2001). For example, the reaction for the CO_2 hydration can be independently written in two forms for ^{12}C and ^{13}C isotopes:

$$^{12}CO_2 + H_2O \underset{^{12}k_-}{\overset{^{12}k_+}{\rightleftharpoons}} H^{12}CO_3^- + H^+ \tag{2.1}$$

$$^{13}CO_2 + H_2O \underset{^{13}k_-}{\overset{^{13}k_+}{\rightleftharpoons}} H^{13}CO_3^- + H^+ \tag{2.2}$$

If the reaction rate constant for CO_2 hydration involving $^{12}CO_2$ ($^{12}k_+$) is greater than the other counterpart for $^{13}CO_2$ ($^{13}k_+$), the reaction product HCO_3^- will be depleted in ^{13}C with respect to the $CO_{2\,(aq)}$ as a result of KIEs for the CO_2 hydration reaction, which is given by $^{12}k_+/^{13}k_+$ (also note the KIE for the reverse reaction, or HCO_3^- dehydration is given by $^{12}k_-/^{13}k_-$). Furthermore, KIE and the equilibrium fractionation (α) for the same chemical reaction is related by:

$$\frac{^{13}K'}{^{12}K} = \alpha = \left(\frac{^{13}k'_{+}}{^{13}k'_{-}}\right)\left(\frac{^{12}k_{-}}{^{12}k_{+}}\right) \quad (2.3)$$

where K and K' are equilibrium constants for the reactions of ^{12}C and ^{13}C, respectively (Eq. (2.1) and (2.2); Zeebe and Wolf-Gladrow, 2001). Also note that rate laws (Eq. (2.1) and (2.2)) as well as the definition of KIE illustrated above can be analogously written for oxygen isotopes ^{16}O and ^{18}O, where KIE for CO_2 hydration is given by $^{16}k_{+}/^{18}k_{+}$. In the remaining text, KIEs in terms of carbon and oxygen isotopes is denoted as ^{13}KIE and ^{18}KIE, respectively.

Evidence of KIEs during the hydration of CO_2 have been observed in various marine processes such as, in speleothem calcites, during the formation of cryogenic carbonates, skeletal formation in corals, and more (Swart, 1983; Adkins et al., 2003; Mickler et al., 2004; Mickler et al., 2006; Daëron et al., 2019). Yet, to date, KIEs for CO_2 hydration are not well constrained in terms of both carbon and oxygen isotopes, which is exemplified by the inconsistencies in the proposed magnitude of KIEs reported in previous experimental and theoretical studies (Marlier and O'Leary, 1984; Clark and Lauriol, 1992; Guo, 2008; Zeebe, 2014; Sade and Halevy, 2017).

One study by Clark and Lauriol (1992) experimentally grew cryogenic calcite and determined carbon and oxygen kinetic isotope fractionation (^{13}KIF and ^{18}KIF) associated with HCO_3^- dehydration to be ~ 32.0‰ and ~ 6‰, respectively, at 0°C. Provided with the carbon and oxygen equilibrium fractionation factors ($^{13}\alpha$ and $^{18}\alpha$) (Zhang et al., 1995 and Beck et al., 2005) and the KIEs for HCO_3^- dehydration determined by Clark and Lauriol, ^{13}KIE and ^{18}KIE during CO_2 hydration can be calculated as 19.7‰ and 3.7‰, respectively, based on the relationship given by Eq. (2.3) (Zeebe, 2014; Sade and Halevy, 2017). However, the mineralogical formation of cryogenic calcite is uncertain, so the KIEs Clark and Lauriol originally calculated may not be characteristic of calcite but rather another type of polymorph such as vaterite or ikaite (Lacella et

al., 2009; Sade and Halevy, 2017). A second experimental study, Marlier and O'Leary (1984) developed methods to determine ^{13}KIEs during CO_2 hydration and HCO_3^- dehydration. For CO_2 hydration, phosphoenolpyruvate (PEP) carboxylase was used to catalyze rapid precipitation of HCO_3^- to form malate. For HCO_3^- dehydration, CO_2 degassed from buffered $NaHCO_3$ solution by helium sweeping was trapped using liquid nitrogen. Based on subsequent isotope analyses on the resultant malate and CO_2 gas, they reported a ^{13}KIF during CO_2 hydration of ~6.9‰ at 24°C. However, in a subsequent study performed by the same group (O'Leary et al., 1992), the ^{13}KIF is oddly reported as 13‰, not 6.9‰ with no further explanation.

Theoretical calculations have also been employed to quantify KIEs associated with CO_2 hydration. Guo (2008) theoretically calculated the ^{18}KIF during HCO_3^- dehydration and reported an ^{18}O depletion in CO_2 relative to HCO_3^- of ~7‰ at 25°C. Sade and Halevy (2017;2018) reported a ^{18}KIF during CO_2 hydration of ~16.4‰ using the relationship between ^{18}KIF for HCO_3^- dehydration reported by Guo (2008) and $^{18}\alpha$ from Beck et al. (2005). However, a more recent theoretical study by Guo and Zhou (2019) reported an estimated ^{18}KIF for the hydration of CO_2 of 4.3‰ at 25°C. Zeebe (2014) reported ^{13}KIF and ^{18}KIF at 25°C to be between ~ 23 and 33‰ and ~13 and 15‰, respectively. These values were based on theoretical calculations where it was assumed that the hydration of CO_2 proceeds in a stepwise fashion through a $HCO_3^- - H_3O^+$ intermediate state rather than directly to the product (H_2CO_3), with each pathway leading to different KIFs (for review, see Section 2.2 or Zeebe, 2014). However, whether or not the CO_2 hydration reaction follows a direct or stepwise pathway is still uncertain. The ^{18}KIFs by Zeebe (2014) reported were calculated using H_2CO_3 as the product of CO_2 hydration and compared the isotopic rate constants for CO_2 hydration to the fractionation between instantaneously produced H_2CO_3 and CO_2 in isotopic equilibrium with H_2O. However, Sade and Halevy (2017; 2018)

separated the individual components of the equilibrium fractionation factor (i.e. CO_2 and H_2O) to calculate the ^{18}KIF between HCO_3^- relative to CO_2 and H_2O as two separate ^{18}KIFs. The revised ^{18}KIFs reported by Sade and Halevy for HCO_3^- relative to CO_2 and HCO_3^- relative to H_2O is between 4.3 and 6.2‰ and 0 to 9.6‰, respectively.

McConnaughey (1989) conducted calcite precipitation experiments in an attempt to replicate kinetic isotope disequilibrium observed in biogenic carbonates. Although his experimental data at 21°C show ^{18}O and ^{13}C depletions of ~5‰ and ~8.3‰ relative to $\delta^{13}C$ and $\delta^{18}O$ values estimated for CO_2 in isotopic equilibrium with Galapagos seawater, we have concerns for the values derived from McConnaughey's precipitation experiments. First, there was no control on solution pH, such that it varied between pH 7.4 and 8.5 during $CaCO_3$ precipitation. Controlling the solution pH is critical because it dictates whether CO_2 hydration (predominant at low pH) or CO_2 hydroxylation (predominant at high pH) is the primary reaction during precipitation. Thus, there is a chance that McConnaughey's (1989) experimental carbonates do not fully record the KIE associated with CO_2 hydration. Second, the ^{13}C and ^{18}O depletions of McConnaughey's experimental $CaCO_3$ were scaled relative to the $\delta^{13}C$ and $\delta^{18}O$ value of the CO_2 source gas. However, the actual $\delta^{13}C$ and $\delta^{18}O$ values of the CO_2 source gas were never provided, which makes it difficult to determine the ^{13}C and ^{18}O partitioning specific to the $CO_{2\,(g)}$-DIC-H_2O system in his study. More details about McConnaughey (1989) will be discussed further in Section 5.

In summary, the currently available experimental data is limited to a few studies and carbon and oxygen KIFs reported in the current literature are inconsistent between experimental and theoretical studies (Table 2.1). The scarcity of available data and notably large inconsistency

therein (e.g. by a factor of ~5; see Table 2.1) suggest more experimental work is required in order to determine the KIE and fully understand the CO_2 hydration/dehydration mechanism.

In this study, we conducted laboratory experiments to constrain kinetic isotope fractionation factors during CO_2 hydration. The experimental setup used in this study was adapted from McConnaughey (1989) but with important modifications that will be discussed in detail in Section 3. We report the results from our carbonate precipitation experiments, which will help define the magnitude of KIFs during CO_2 hydration. The results reported here will also provide the experimental data necessary to evaluate the accuracy of theoretical calculations, which have yet to be confirmed by experimental data.

Table 2.1. The average ^{13}KIFs and ^{18}KIFs of CO_2 hydration reported from previous experimental and theoretical studies.

Reference	T (°C)	(E)xperimental/(T)heoretical	$^{13}KIF_{CO_2-HCO_3^-}$ (‰)	$^{18}KIF_{CO_2-HCO_3^-}$ (‰)
Clark & Lauriol (1992)	0	E	19.7	3.7*
Marlier & O'Leary (1984)	24	E	6.9	--
O'Leary et al. (1992)	24	E	13	--
McConnaughey (1989)	21	E	8.3	5
Zeebe (2014)	25	T	23-33 ($n \geq 4$)	13-15 ($n \geq 4$)[a]
Zeebe (2014)			10-14($n \leq 3$)	10.5-15 ($n \leq 3$)
	25	T	--	5.2*
Guo (2008)	0	T	--	16.4
Guo & Zhou (2019)	25	T		4.3

*The values reevaluated by Sade and Halevy (2017 and 2018).
[a]KIF between $CO_{2(g)}$ and H_2CO_3

2. THEORY

The reaction mechanism for the hydration of CO_2 and dehydration of HCO_3^- can be written as (Eigen et al., 1961; Zeebe and Wolf-Gladrow, 2001):

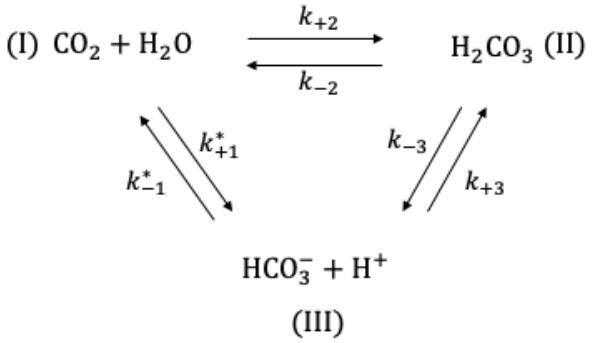

(2.4)

where the $k_{\pm}$'s are the reaction rate constants and the overall rate constant is $k = k^*_{+1} + k_{+2}$. It has been demonstrated through quantum chemistry calculations that the two reaction pathways (i.e. [(I)→(II)→(III)] and [(I)→(III)]) are likely associated with two different reaction mechanisms leading to different KIEs for both carbon and oxygen (Zeebe, 2014). However, there is an ongoing debate as to whether HCO_3^- forms directly following a concerted pathway (I→III) or if the reaction proceeds to H_2CO_3 in a stepwise fashion via $HCO_3^- - H_3O^+$ intermediate state (I→II→III) (Nguyen et al., 2008; Stirling and Papai, 2010; B. Wang and Cao, 2013; Zeebe, 2014). Thus, placing accurate constraints on the KIEs for CO_2 hydration could even reconcile the reaction pathways and molecular mechanisms of CO_2 hydration. For this study we define the CO_2 hydration/dehydration reaction as:

$$CO_2 + H_2O \rightleftharpoons HCO_3^- + H^+ \quad (2.5)$$

Eq. (2.5) is the predominant reaction that occurs at pH ≤ 8.5 (McConnaughey, 1989; Johnson, 1982), while at pH ≤ 8.5 the concentration of hydroxyl ions (OH^-) increases and favors the hydroxylation/dehydroxylation reaction:

$$CO_2 + OH^- \rightleftharpoons HCO_3^- \quad (2.6)$$

The hydration and hydroxylation reaction (Eq. (2.5) and (2.6), respectively) are associated with different KIEs, so controlling the pH is critical to successfully determine KIF during CO_2 hydration (Johnson, 1982; McConnaughey, 1989; Guo, 2008; Sade and Halevy, 2017). KIEs of carbon and oxygen during CO_2 hydration can be determined by comparing $\delta^{13}C$ and $\delta^{18}O$ values of experimental HCO_3^- (via quantitative transformation into $BaCO_3$) to the $\delta^{13}C$ and $\delta^{18}O$ values of $CO_{2\,(g)}$ and instantaneously formed HCO_3^-, in which the latter $\delta^{13}C$ and $\delta^{18}O$ values are constrained from equilibrium ^{13}C and ^{18}O partitioning in the $CO_{2\,(g)}$ – DIC – H_2O system calculated from well-known ε (Brenninkmeijer et al., 1983; Zhang et al., 1995). If KIEs exist, the $\delta^{13}C$ and $\delta^{18}O$ values of $BaCO_3$ will be different from those of equilibrium of CO_2 and instantaneously formed HCO_3^-. The lower $\delta^{13}C$ and $\delta^{18}O$ values of the product (i.e. experimental $BaCO_3$) than that of equilibrium $CO_{2\,(g)}$ and instantaneously formed HCO_3^-, suggests the reaction rate of the lighter ^{12}C and ^{16}O isotopes is greater than the reaction rate of the heavier ^{13}C and ^{18}O isotopes. As a result of the lighter isotopes having a greater reaction rate, ^{12}C and ^{16}O will be preferentially incorporated in the product (HCO_3^- and hence, $BaCO_3$), while ^{13}C and ^{18}O will be enriched in the unreacted reactant (CO_2). We define KIFs here by the ^{13}C and ^{18}O depletions observed in $BaCO_3$ relative to equilibrium $CO_{2\,(g)}$ and instantaneously

formed HCO_3^-. Sections 2.1 and 2.2 will discuss the relevant equilibrium reaction sequences for both carbon and oxygen, the theoretical calculations used to determine the stable isotope values of equilibrium DIC components, and the equations used to calculate ^{13}KIF and ^{18}KIF.

2.1 Carbon Isotope Fractionation

In our experimental setup, $CO_{2\,(g)}$ is liberated from a $NaHCO_3$ stock solution and circulated throughout the system until it is isotopically equilibrated with the $NaHCO_3$ stock solution reservoir (further described in Section 3). The $^{13}\varepsilon$ between $CO_{2\,(g)}$ and HCO_3^- (Eq. (2.5)) is known and can be used in combination with the measured δ^{13}C value of $NaHCO_3$ $\left(\delta^{13}C_{NaHCO_3\,(VPDB)} = -2.8 \pm 0.16‰\right)$ to calculate the δ^{13}C value of $CO_{2\,(g)}$. The $^{13}\varepsilon$ between $CO_{2\,(g)}$ and HCO_3^- was reported as a function of temperature by Zhang et al. (1995) as:

$$^{13}\varepsilon_{(HCO_3^- - CO_{2\,(g)})} = (-0.1141 \pm 0.0028)(T_{°C}) + (10.78 \pm 0.04‰) \quad (2.7)$$

where T_c is the temperature in °C at which the reaction occurs ($^{13}\varepsilon_{(HCO_3^- - CO_{2\,(g)})} = 7.9 \pm 0.04‰$ (VPDB) at T=25°C). By substituting $^{13}\varepsilon_{(HCO_3^- - CO_{2\,(g)})}$ and the measured δ^{13}C of $NaHCO_3$, the δ^{13}C value of $CO_{2\,(g)}$ in equilibrium with HCO_3^- can be determined. Changes in temperature affect the magnitude of $^{13}\varepsilon_{(HCO_3^- - CO_{2\,(g)})}$ in an anticorrelated fashion such that, fractionation increases with decreasing temperatures and decreases as temperatures increase ($^{13}\varepsilon_{(HCO_3^- - CO_{2\,(g)})} \approx 10.8$ and 6.8‰ at T=0° and 35°C, respectively; Zhang et al., 1995; Zeebe and Wolf-Gladrow, 2001).

We define our experimental ^{13}KIF for the remainder of this study to be between equilibrium $CO_{2\ (g)}$ and experimental $BaCO_3$ which can be calculated from the equation:

$$^{13}\mathrm{KIF}=\frac{\delta^{13}C_{CO_{2\ (g)}}+1000}{\delta^{13}C_{BaCO_3}+1000} \tag{2.8}$$

where ^{13}KIF reports the magnitude of the observed isotope fractionation between equilibrium $CO_{2\ (g)}$ and experimental $BaCO_3$, which will be reported in per mil (‰; i.e. (^{13}KIF-1)*1000).

2.2 Oxygen Isotope Fractionation

Constraining the equilibrium oxygen isotope partitioning in the $CO_2 - H_2O$ system is slightly more complex than that of carbon. The relevant equilibrium reactions associated with oxygen isotope equilibration include Eq. (2.5) and (2.6), and the equilibrium reaction between gaseous CO_2 and H_2O:

$$CO_{2\ (g)} \rightleftharpoons H_2O \tag{2.9}$$

Although, the oxygen isotope composition of $CO_{2\ (g)}$ ($\delta^{18}O_{CO_{2\ (g)\ (vs.\ VSMOW)}}$) was not directly measured in this study, but can be determined from the equation provided by Brenninkmeijer et al. (1983) for $^{18}\alpha$ of $CO_{2\ (g)}$ relative to H_2O:

$$^{18}\alpha_{(CO_{2(g)}\text{-}H_2O_{(l)})}=\frac{17.604}{T}+0.98211\ (\pm\ 0.00005) \tag{2.10}$$

where T is the temperature in Kelvin ($^{18}\alpha_{(CO_{2(g)}\text{-}H_2O_{(l)})} = 1.04115$ or $^{18}\varepsilon_{(CO_{2(g)}\text{-}H_2O_{(l)})} = 41.2‰$ at T=25°C). The unknown value of $\delta^{18}O_{CO_{2\,(g)}\,(vs.\ VSMOW)}$ can be derived by the relationship between $^{18}\alpha_{(CO_{2(g)}\text{-}H_2O(l))}$ and the measured $\delta^{18}O_{H_2O\,(vs.\ VSMOW)}$ ($\delta^{18}O_{H_2O\,(vs.\ VSMOW)} = -3.1 \pm 0.04‰$). Reactant ratios (i.e. $^{18}R_{CO_{2\,(g)}}$ and $^{18}R_{H_2O}$) can be used to determine the isotope ratio of HCO_3^- ($^{18}R_{HCO_3^-}$) instantaneously produced from the reaction between $CO_{2\,(g)}$ and H_2O (McConnaughey, 1989; McConnaughey, 2003; Zeebe, 2014):

$$^{18}R_{HCO_3^-} = \frac{2}{3}\ ^{18}R_{CO_{2(g)}} + \frac{1}{3}\ ^{18}R_{H_2O} \tag{2.11}$$

where $^{18}R_{HCO_3^-}$ is the isotope ratio of HCO_3^- instantaneously produced from $CO_2 + H_2O$ without fractionation.

We define our experimental ^{18}KIF for the remainder of this study to be between instantaneously formed HCO_3^- (Eq. (2.11)) and experimental $BaCO_3$ calculated by the equation:

$$^{18}\text{KIF} = \frac{\delta^{18}O_{\text{instant } HCO_3^-} + 1000}{\delta^{18}O_{BaCO_3} + 1000} \tag{2.12}$$

where ^{18}KIF represents the magnitude of the observed fractionation between instantaneously formed HCO_3^- and experimental $BaCO_3$ given in per mil (‰; i.e. (^{18}KIF-1)*1000).

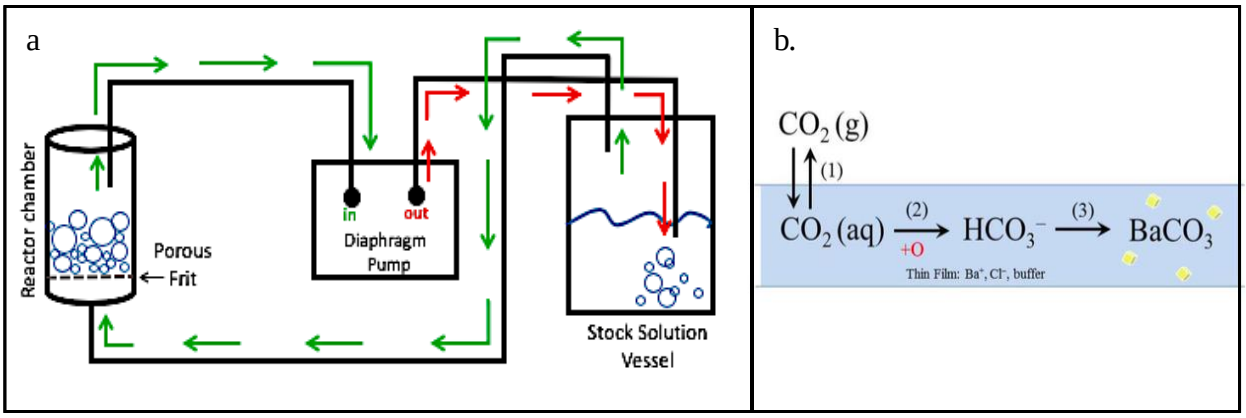

Fig. 2.1. a) Schematic view of the experimental setup used in this study. The setup allows continuous transfer of internal gas through the stock solution vessel and reactor chamber in a closed circuit by a diaphragm pump. All components are connected by flexible and gas-impermeable tubes. b) A cross-section across the gas-solution interface during the precipitation of $BaCO_3$, where the thin film of the bubbles produced in the reactor chamber above the frit is shown in blue. Labels (1), (2), and (3), indicate the steps that can cause isotope fractionation. (1) $CO_{2\ (g)}$ diffuses across the thin film, (2) the hydration/hydroxylation of $CO_{2\ (aq)}$, where an additional oxygen (shown in red) is derived from either H_2O or OH^-, and (3) $BaCO_3$ precipitation. Step (2) is the isotope fractionation during CO_2 hydration/hydroxylation that we aim to capture with this experimental system.

3. METHODS

3.1 Overview of the Experimental Approach

We used an experimental approach similar to the methods described by McConnaughey (1989), but with important modifications (Fig. 2.1a). To test for KIEs, we first established full isotopic equilibrium between $CO_{2\ (g)}$ and the $NaHCO_3$ stock solution (see Section 3.3). Once isotopic equilibrium was established, the $CO_{2\ (g)}$ bubbled through a buffered $BaCl_2$ solution (i.e. the reactor solution). The thin liquid film surrounding the bubbles allowed $CO_{2\ (g)}$ to diffuse across the gas-liquid interface (Fig. 2.1b). Upon the hydration of $CO_{2\ (aq)}$, all of the HCO_3^- formed in solution was quantitatively removed from solution by immediately reacting with Ba^{2+} to form solid $BaCO_3$ precipitates. Use of a buffer in the reactor solution minimized pH change upon

$BaCO_3$ precipitation, an important modification from McConnaughey (1989), as pH dictates hydration/hydroxylation.

Equilibrium partitioning of carbon and oxygen isotopes between $CO_{2\,(g)}$ and $NaHCO_3$ was constrained from measured $\delta^{13}C$ and $\delta^{18}O$ values of $NaHCO_3$ and H_2O as well as the relevant equilibrium fractionation factors discussed in Section 2. Thus, the $\delta^{13}C$ values of bubbling $CO_{2\,(g)}$ and $\delta^{18}O$ values of instantaneously-formed HCO_3^- (from Eq. (2.10)) was precisely known, which represents another improvement compared to the methods used by McConnaughey (1989). With this information, we can quantify KIFs for CO_2 hydration as the offsets between $\delta^{13}C_{BaCO_3}$ and $\delta^{13}C_{CO_{2\,(g)}}$, and $\delta^{18}O_{BaCO_3}$ and $\delta^{18}O_{HCO_3^-}$.

3.2 Experimental Setup

The setup consisted of two separate containers, a stock solution vessel and a reaction chamber, which are connected with gas-impermeable C-Flex tubing and a fully sealed diaphragm pump (Single-head Air Cadet; Fig. 2.1b.). To control the temperature of the experiment, the stock solution vessel was placed inside of a temperature-controlled water bath throughout the duration of the experiment. A thermometer was placed inside of the reactor chamber and a temperature controlled wrap was placed around the reactor until the desired temperature was reached. The reactor chamber was equipped with a pair of air ports located on the top and bottom of the 1L vessel. Placed on the bottom of the reactor chamber was a fritted disk with 25-50μm porosity (designation C) that allowed internal gas to pass through. The reactor chamber was initially free of any solution during the gas equilibration period. The top of the stock solution vessel was sealed with a rubber stopper to which two air tight tube connections were attached. The bottom port of the reactor chamber was connected to one of the tubes atop the stock solution

vessel through which internal gas from the headspace of the stock solution vessel flowed to the bottom port of the reactor. The second tube on the stock solution vessel was connected to the pressure port of the diaphragm pump. The tube connected to the pump extended into the stock solution vessel through which internal air continuously bubbled the stock solution (the CO_2 source). The pump vacuum port (in flow) was connected to the leak proof rubber stopper on top of the reactor chamber, which pulled the internal gas into the pump and allowed the gas to continuously circulate throughout the entire system until complete C and O isotope equilibrium in the $CO_{2\ (g)}$-DIC-H_2O system was established.

3.3 Experimental Procedures

The $NaHCO_3$ stock solution was prepared to a concentration of 1M (pH 7.9) by dissolving isotopically homogenous $NaHCO_3$ powder ($\delta^{13}C_{VPDB}$ = -2.8 ± 0.08‰, $\delta^{18}O_{VSMOW}$ = 14.5 ± 0.09‰, 1σ S.D., pH 7.9, n=8; Certified A.C.S. grade: Fisher Lot#177037) into Milli-Q ultra-pure deionized water of known isotopic composition (D.I. H_2O; $\delta^{18}O_{VSMOW}$ = -3.1 ± 0.04‰, 1σ S.D., n=5). It is important to note that the $\delta^{18}O_{VSMOW}$ of the D.I. H_2O was constant throughout the study period and the same D.I. H_2O source was used for all aspects of the experiments.

The reactor solution was prepared by dissolving barium chloride dihydrate ($BaCl_2 \bullet 2H_2O$) crystals (Reagent A.C.S. grade: J.T. Baker #H10587) into 20mL of 0.4 M TRIS ($NH_2C(CH_2OH)_3$) buffer solution. Prior to making the reactor solution, the Tris buffer was adjusted to the desired pH values by titration with 1N HCl, during which pH was monitored by a benchtop pH meter (Thermo Scientific Orion 3-Star model) equipped with an AccuTupH electrode (Cole Parmer #55501-02). The pH electrode was calibrated before every use using

Orion pH buffers (pH 4.01, 7.00, 10.01) that are traceable to NIST standard reference material. Note that the prepared Tris buffer was maintained at experimental temperatures by storing it in the same water bath where the stock solution vessel was placed. Finally, ~488.52 mg of $BaCl_2 \bullet 2H_2O$ crystals were dissolved into 20 mL of the Tris buffer to yield a 0.1M concentration immediately before injection into the reactor chamber to ensure no precipitants formed prior to entering the system. To ensure precipitation of $BaCO_3$ was indeed quantitative and prevent re-equilibration between HCO_3^- and dissolved $CO_{2\ (aq)}$, we compared the initial moles of barium (Ba) in the reactor solution to the moles of Ba precipitated out of solution as $BaCO_3$. If the initial moles of Ba is greater than the moles of Ba in the precipitated $BaCO_3$, then it can be said that precipitation of $BaCO_3$ was quantitative.

Prior to introducing the Tris+$BaCl_2$ reactor solution for $BaCO_3$ precipitation, the internal CO_2 gas was circulated throughout the system for a minimum of 16 hours, which is theoretically sufficient to establish full carbon and oxygen isotope equilibrium in the $CO_{2\ (g)}$-DIC-H_2O system at our experimental conditions (see Eq. (A1-a) and Eq. (A1-b) in Appendix; Zeebe and Wolf-Gladrow, 2001; Usdowski et al., 1991). Once the equilibration time elapsed, the reactor solution was dispensed into the reactor chamber through an injection port located on top of the chamber using a syringe. The reactor solution sat above the fritted disk inside the reactor chamber where it bubbled for two minutes. Fig. 2.1b illustrates the cross section of the thin gas-liquid interface produced from the bubbles and the steps at which isotope fractionation can occur during the transformation from $CO_{2\ (g)}$ to solid $BaCO_3$. The isotope fractionation during CO_2 hydration/hydroxylation (Step (2) from Fig. 2.1b) is the fractionation we aim to capture by immediately precipitating HCO_3^- as solid carbonate (i.e. $BaCO_3$).

The $BaCO_3$ precipitates formed during the two minutes of bubbling were quickly removed from the reactor and filtered onto a 0.45 μm cellulose ester membrane filter, followed by a rigorous D.I. H_2O rinse. After filtration, the $BaCO_3$ collected onto the filter was oven-dried at approximately 65°C overnight. Once precipitates were completely dried, the samples were homogenized and stored in glass vials until stable isotope analyses. Each precipitation experiment was performed in duplicate to account for reproducibility. Experiments were separated into 4 batches with slightly different conditions described in Table 2.2. For a full description of all of the different parameter runs refer to Table A1 in the Appendix.

Table 2.2. Parameter descriptions of the 4 batches of experiments, including the total number of experiments per batch and the time frame at which each batch was ran. The pH was measured in the tris buffer/reactor solution.

Batch #	Date of Experiments	Total	T (°C)	pH	[$BaCl_2$] (mol L^{-1})
1	August 2017 – October 2017	15	21	8.2 (n=13) 10.3 (n=2)	0.1 (n=11) 0.2 (n=2) 0.3 (n=2)
2	December 2017 – February 2018	8	21	8.0 (n=6) 9.0 (n=2)	0.1
3	April 2018 – July 2018	22	25 (n=19), 30 (n=3)	7.5 (n=5) 8.5 (n=10) 9.0 (n=2) 9.2 (n=2) 9.5 (n=2)	0.1 (n=20) 0.2 (n=2)
4	July 2018 – November 2018	12	18 (n=2), 25 (n=10)	8.0	0.1

3.4 Stable Isotope Analyses

Stable isotopes are measured and reported on the conventional delta notation. Barium carbonate samples were sent to the University of California, Santa Cruz Stable Isotope Laboratory to be analyzed for stable carbon and oxygen isotopes. Approximately 60μg aliquots of homogenized samples were analyzed by conventional acid digestion using

ThermoScientificKiel IV carbonate device coupled to a ThermoScientific MAT-253 dual-inlet isotope ratio mass spectrometer (IRMS). During the analysis, samples are reacted with H_3PO_4 orthophosphoric acid (specific gravity = 1.92g/cm^3) at 75°C to produce CO_2 from $BaCO_3$. The H_2O produced is then cryogenically separated and non-condensable gases are removed prior to introduction of CO_2 analyte into the IRMS. All samples were analyzed with several replicates of the externally calibrated in-house standard reference material (CM12) and the NBS-18 limestone international standard reference material for a drift correction. Two natural samples of 'Atlantis II' powdered coral are run daily to monitor operational performance. Typical reproducibility of replicate $\delta^{13}C$ and $\delta^{18}O$ measurements on the NBS-18 standards were better than $\pm$ 0.05‰ and $\pm$ 0.10‰ ($\pm 1\sigma$), respectively. The NBS-18 standard has the assigned $\delta^{18}O$ value of -23.2‰ relative to VPDB which is established by applying a correction derived from comparing the $\delta^{18}O$ of the CO_2 liberated from NBS-18 via phosphoric acid digestion and the CO_2 reference gas. Because this cross-referencing method is used, the $BaCO_3$ acid fractionation factor is not applied (Böttcher, 1996). Measured $\delta^{13}C$ and $\delta^{18}O$ values of $BaCO_3$ samples were reported on the VPDB-scale, however, for calculating ^{18}KIF, $\delta^{18}O$ values had to be re-scaled to VSMOW using the equation given by Coplen et al. (1983):

$$\delta^{18}O_{VSMOW} = 1.03091 \times \delta^{18}O_{VPDB} + 30.91‰ \quad (2.13)$$

Here, we report all $\delta^{18}O$ values will be reported relative to VSMOW and all $\delta^{13}C$ values will be reported relative to VPDB.

Deionized H_2O samples were analyzed for $\delta^{18}O$ at the Stable Isotope Biogeochemistry (SIB) Lab located at the University of Hawaii at Manoa on a fully-automated Picarro L2130-i

WS-CRDS cavity ring-down spectrometer fitted with an A0211 High Precision Vaporizer and HTC PAL autosampler. Results were normalized to VSMOW using the following three in-house reference materials: desalinated deep seawater (KONA; $\delta^{18}O = 0.51‰$) laboratory deionized water (LAB DI; $\delta^{18}O = -5.11‰$), and melted snow collected from Mauna Kea summit (MKSNOW; $\delta^{18}O = -13.44‰$). The final results were reported using δ notation in permil (‰) relative to VSMOW. The in-house reference materials were extensively calibrated against NIST reference materials (including Standard Light Antarctic Precipitation-2 (SLAP-2), Vienna Standard Mean Ocean Water-20 (VSMOW-2), and Greenland Ice Sheet Precipitation (GISP) from the International Atomic Energy Agency (Vienna, Austria). Accuracy and precision of analysis was determined by repeated analysis of Evian bottled water and was found to be within accuracy capabilities of the instrument reported by the manufacturer ($\delta^{18}O = 0.2‰$). Sample precision for $\delta^{18}O$ values of our D.I. H_2O samples at 1 standard deviation was 0.03‰ from n=5 D.I. H_2O samples.

4. RESULTS

4.1 Isotopic Equilibrium of DIC Species in the Carbonate System

As discussed in Section 3, equilibrium partitioning of C and O isotopes must be constrained to calculate equilibrium $\delta^{13}C$ and $\delta^{18}O$ values of the compounds that were not directly measured in the $CO_{2\,(g)}$-DIC-H_2O system. For easier comparison, all equilibrium isotope fractionation factors for the remainder of the text will be expressed in permil (‰) and denoted as ε. Fig. 2.2 compares the carbon and oxygen equilibrium isotope values calculated from Eq. (2.7), (2.10), and (2.11) to the mean $\delta^{13}C$ and $\delta^{18}O$ values of Batch-4 $BaCO_3$ to illustrate KIF during CO_2 hydration (Eq. (2.8) and Eq. (2.12)).

The $^{13}\varepsilon$ between HCO_3^- and $CO_{2\,(g)}$ ($^{13}\varepsilon_{HCO_3^-\text{-}CO_{2(g)}}$) calculated from Eq. (2.7) is ~8 $\pm$ 0.04‰ at 25°C, where the $\delta^{13}C$ value of equilibrium HCO_3^- is isotopically lighter than the $\delta^{13}C$ value of equilibrium $CO_{2\,(g)}$. The $^{13}\varepsilon_{HCO_3^-\text{-}CO_{2(g)}}$ is indicative of the equilibrium fractionation between stock solution $NaHCO_3$ and the $CO_{2\,(g)}$ evolved from the stock solution, which was circulated throughout the system. From the relationship between $^{13}\varepsilon_{HCO_3^-\text{-}CO_2}$ and the $\delta^{13}C$ value measured for $NaHCO_3$, we can derive the $\delta^{13}C$ value of $CO_{2\,(g)}$ from the following equation:

$$\delta^{13}C_{CO_{2\,(g)}} = \frac{\delta^{13}C_{NaHCO_3} - {}^{13}\alpha_{HCO_3^-\text{-}CO_{2\,(g)}}}{\left[\left(\frac{{}^{13}\alpha_{HCO_3^-\text{-}CO_{2\,(g)}}}{1000}\right)+1\right]} \qquad (2.14)$$

where the $\delta^{13}C_{CO_{2\,(g)}} \approx$ -10.7 $\pm$ 0.17‰ at 25°C. Table 2.1 reports the $^{13}\varepsilon$ and the isotopic compositions calculated for $CO_{2\,(g)}$ and DIC species at the different temperatures each experimental batch was performed.

Equilibrium $^{18}\varepsilon_{CO_{2\,(g)}\text{-}H_2O}$ calculated from Eq. (2.10) is 41.2‰, where the $\delta^{18}O$ value of $CO_{2\,(g)}$ (i.e. $\delta^{18}O_{CO_{2(g)}}$) is isotopically heavier relative to the isotopic composition of H_2O. The $\delta^{18}O_{CO_{2(g)}}$ can be calculated using the relationship between $^{18}\varepsilon_{CO_{2\,(g)}\text{-}H_2O}$ and the measured $\delta^{18}O_{H_2O}$ by the equation:

$$\delta^{18}O_{CO_{2\,(g)}} = \left[{}^{18}\alpha_{CO_{2\,(g)}\text{-}H_2O}\cdot(\delta^{18}O_{H_2O}+1000)\right] - 1000 \qquad (2.15)$$

where the $\delta^{18}O_{CO_{2(g)}} \approx 38 \pm 0.49‰$ at 25°C. Using the calculated value for $\delta^{18}O_{CO_{2(g)}}$ and the measured $\delta^{18}O_{H_2O}$, the $\delta^{18}O$ value of HCO_3^- instantaneously produced from CO_2 and H_2O without fractionation was determined from Eq. (2.11) to be ~24.3± 0.49‰ at 25°C (Table 2.3).

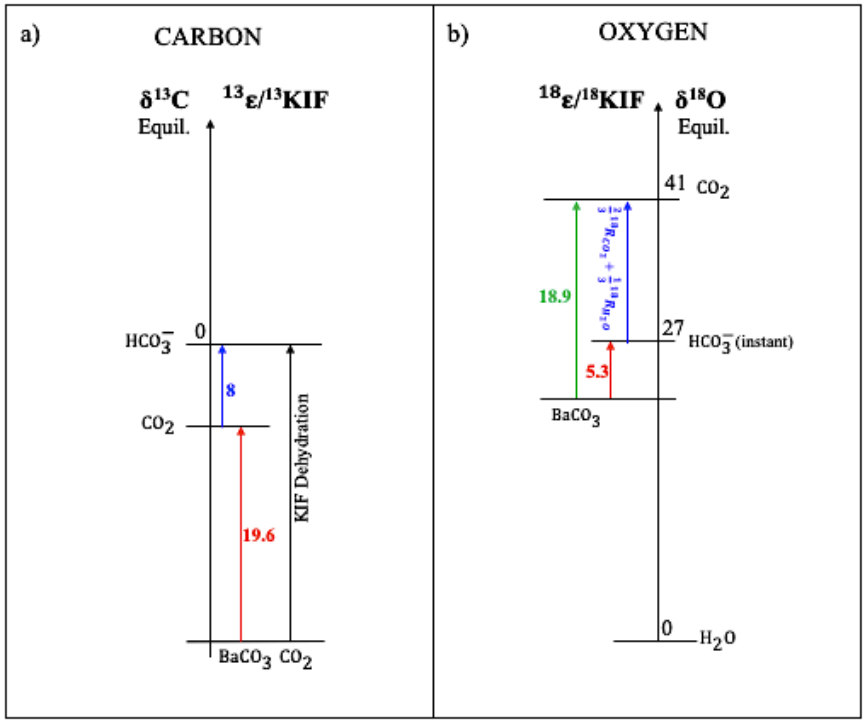

Fig. 2.2. A schematic illustration of carbon and oxygen equilibrium fractionation and KIF during CO_2 hydration at 25°C, where all values are expressed in ‰. a) For carbon, the $\delta^{13}C$ value of HCO_3^- is arbitrarily set to 0‰ on the left of the axis. The $^{13}\varepsilon$ between HCO_3^- and $CO_{2\,(g)}$ is ~8‰ (blue) on the right of the axis, where the blue arrow direction indicates HCO_3^- is isotopically heavier relative to $CO_{2\,(g)}$, which is roughly given by the difference between δ-values (i.e. $^{13}\varepsilon_{HCO_3^- - CO_{2(g)}} \approx \delta^{13}C_{HCO_3^-} - \delta^{13}C_{CO_{2(g)}}$). Similarly, the difference between $\delta^{13}C_{CO_{2(g)}}$ and the mean $\delta^{13}C_{BaCO_3}$ yields the mean ^{13}KIF (19.6±0.25‰; red), where $BaCO_3$ is isotopically lighter relative to $CO_{2\,(g)}$ (red arrow). b) For oxygen, the $\delta^{18}O$ value of H_2O is arbitrarily set to 0‰ and the $\delta^{18}O$ of HCO_3^- instantaneously produced without fractionation from CO_2 and H_2O is 27‰, calculated from Eq. (2.11) (blue arrow). $\delta^{18}O$ values that fall below 27‰ indicate KIEs. The difference between $\delta^{18}O_{HCO_3^-(instant)}$ and the mean $\delta^{18}O_{BaCO_3}$ is equal to the mean ^{18}KIF (5.3±0.55‰; red), where $BaCO_3$ is isotopically lighter relative to $HCO_{3(instant)}^-$ (red arrow). The ^{18}KIF (green) is calculated from the difference between the $\delta^{18}O_{CO_{2(g)}}$ and the mean $\delta^{18}O_{BaCO_3}$ where $BaCO_3$ is isotopically lighter relative to $CO_{2\,(g)}$ (green arrow).

Table 2.3. The equilibrium $^{13}\varepsilon$ and $^{18}\varepsilon$ between the relevant $CO_{2\,(g)}$-DIC-H_2O species estimated based on the temperature dependence of the fractionation factors previously determined. The $\delta^{13}C$ and $\delta^{18}O$ values for $CO_{2\,(g)}$ were constrained from the calculated equilibrium ε, along with the $\delta^{13}C$ of $NaHCO_3$ ($\delta^{13}C$ = -2.8‰ (VPDB)) and $\delta^{18}O$ of H_2O ($\delta^{18}O$ = -3.1 (VSMOW)) directly measured and used for the experiments. The $\delta^{18}O$ value of instant HCO_3^- was calculated from Eq. (15). All ε and δ values are reported in ‰ and temperature is reported in °C.

Batch #	T	$^{13}\varepsilon_{CO_{2\,(g)}-HCO_3^-}$ [a] (±0.04)	$^{18}\varepsilon_{CO_{2\,(g)}-HCO_3^-}$	$^{18}\varepsilon_{CO_{2\,(g)}-H_2O}$ [b] (±0.00005)	$\delta^{13}C_{CO_{2\,(g)}}$	$\delta^{18}O_{CO_{2\,(g)}}$	$\delta^{18}O_{Instant.HCO_3^-}$
1	21	8.3	13.6 ± 0.02	42.0	-11.1 ± 0.18	38.7 ± 0.50	24.8 ± 0.50
2	21	8.3	13.6 ± 0.02	42.0	-11.1 ± 0.18	38.7 ± 0.50	24.8 ± 0.50
3	25	7.9	13.4 ± 0.02	41.2	-10.7 ± 0.17	38.0 ± 0.49	24.3 ± 0.49
	30	7.3	13.0 ± 0.02	40.2	-10.1 ± 0.17	37.0 ± 0.48	23.6 ± 0.48
4	18	8.7	13.8 ± 0.02	42.6	-11.5 ± 0.18	39.3 ± 0.51	25.2 ± 0.51
	25	7.9	13.4 ± 0.02	41.2	-10.7 ± 0.17	38.0 ± 0.49	24.3 ± 0.49

[a] Calculated using the equilibrium fractionation between HCO_3^- and $CO_{2\,(g)}$ given by Zhang et al. (1995) from Eq. (11).
[b] Calculated from the $^{18}\alpha_{CO_{2(g)}-H_2O}$ provided by Brenninkmeijer et al. (1983) from Eq. (14) and converted to a permil value by the equation (α -1)*1000.

4.2 $BaCO_3$ Data

A complete list of sample details and the results of IRMS analysis can be found in Table A1 in the Appendix. The pH described for each batch in the following text refers to the pH of the reactor solution in which the $BaCO_3$ samples were precipitated. The uncertainty for individual samples and its replicate measurement is reported as the $\pm 2\sigma$ S.D. (95% confidence level) of the average measurement for each sample and its duplicate measurement. The uncertainty reported for mean sample measurements represents the standard error of the mean ($\pm\sigma_m$).

The Batch-1 experiments were run at T=21°C and pH at either 8.2 (n=9) or 10.3 (n=2) from August 2017 to October 2017. An average of ~54.6 mg of $BaCO_3$ were produced from these experiments. The moles of Ba in the initial reactor solution and moles of Ba in the final $BaCO_3$ were calculated using the molecular weight of Ba (M.W. Ba = 137.33 g/mole). The initial moles of Ba in the reactor solution had an average of ~4.34 mmol and an average of ~0.40 mmol Ba was calculated from the mass of the final $BaCO_3$ precipitates. The $\delta^{13}C$ values of Batch-1 samples produced at pH 8.2 ranged from -30.2 ± 0.06 to -27.7 ± 0.27‰ with mean of -

28.9 ± 0.56‰, whereas $\delta^{18}O$ ranged from 18.9 ± 0.12 to 20.0 ± 0.04‰ with an average of 19.6 ± 0.25‰ at the same pH. The $BaCO_3$ samples produced at pH 10.3 (n=2) had $\delta^{13}C$ values that range between -26.2 ± 0.21 to -25.0 ± 1.73‰ with a mean $\delta^{13}C$ value of -25.6 ± 1.26‰. The $\delta^{18}O$ values of $BaCO_3$ samples produced at pH 10.3 range from 15.5 ± 0.21 to 16.4 ± 3.45‰ with a mean $\delta^{18}O$ value of 15.9 ± 0.92‰.

Batch-2 experiments (n=6) ran at T=21°C and pH 8.0 from December 2017 to February 2018 produced typical $BaCO_3$ yields of ~58.2 mg. The initial moles of Ba in the reactor solution had an average of ~3.54 mmol and an average of ~0.42 mmol Ba was calculated from the mass of the final $BaCO_3$ precipitates. The $\delta^{13}C$ values of Batch-2 samples produced at pH 8.0 ranged from -28.9 ± 1.29 to -30.8 ± 0.08‰ with a mean value of -30.2 ± 0.79‰. For oxygen, $\delta^{18}O$ values ranged from 16.0 ± 0.03 to 17.4 ± 0.45‰ with a mean value of 17.0 ± 0.45‰. The $\delta^{13}C$ and $\delta^{18}O$ values of Batch-2 experiments produced at pH 9 (n=2) ranged between -31.2 ± 0.54 to -19.7 ± 3.76‰ with a mean of -25.4 ± 11.52‰ and 14.2 ± 0.03 to 15.4 ± 0.12‰ with a mean of 14.8 ± 1.23‰, respectively.

Batch-3 experiments were ran at several pH and two different temperatures between April 2018 to July 2018, with a total of 22 experiments (see Appendix for all Batch-3 results). An average of ~64.1 mg of $BaCO_3$ was produced in these experiments (n=22). The initial moles of Ba in the reactor solution had an average of ~3.91 mmol and an average of ~0.47 mmol Ba was calculated from the mass of the final Batch-3 $BaCO_3$ precipitates. For experiments that were ran at T=30° and pH 8.5 (n=3) $\delta^{13}C$ values ranged from -29.9 ± 0.83‰ to -27.8 ± 0.16‰ with a mean value of -28.7 ± 1.26‰. and were run at T=25°C and pH 8.5 from April 2018 to July 2018. The $\delta^{13}C$ values of $BaCO_3$ samples produced at T=25°C and pH 8.5 (n=7) ranged from -30.9 ±

0.75 to -23.1 ± 0.47‰, with a mean value of -27.9 ± 2.49‰, whereas $\delta^{18}O$ values ranged from 15.0 ± 0.07 to 17.2 ± 0.10‰, with a mean value of 16.3 ± 0.64‰. Batch-3 samples produced at pH ≥ 9 (n=7) had $\delta^{13}C$ values that range between -31.7 ± 0.04 to -23.0 ± 0.12‰ with a mean of -28.0 ± 4.59‰ and $\delta^{18}O$ values that range between 13.2 ± 0.01 to 16.0 ± 0.05‰ with a mean value of 14.1 ± 1.38‰. A more detailed report of Batch-3 data including specific pH is reported in Table A1 located in the Appendix. Some of the data from Batches 1, 2, and 3 had issues (discussed further in Section 5) and hence are not used to constrain KIEs, these data can also be found in Table A1 in the Appendix.

Batch-4 experiments were ran at pH 8.0 and either T=25°C (n=10) or 18°C (n=2) between July 2018 to November 2018. The average amount of $BaCO_3$ produced in these experiments was ~46.8 mg. The initial moles of Ba in the reactor solution had an average of ~3.58 mmol and an average of ~0.34 mmol Ba was calculated from the average mass of the final Batch-4 $BaCO_3$ precipitates (n=12). The $\delta^{13}C$ values of $BaCO_3$ samples produced at T=25°C and pH 8.0 (n=10) ranged from -32.2 ± 0.22 to -27.8 ± 0.02‰ (Fig. 2.3) with a mean value of -29.7 ± 0.71‰, and the $\delta^{18}O$ values of the same $BaCO_3$ samples ranged from 17.2 ± 0.04 to 20.1 ± 0.21‰ (Fig. 2.3) with a mean value of 18.9 ± 0.56‰.The $\delta^{13}C$ values of $BaCO_3$ samples produced at T=18°C and pH 8.0 (n=2) ranged from -30.5 ± 0.14 and -31.8 ± 0.20‰ with a mean value of -31.1 ± 1.26‰, while the $\delta^{18}O$ values of the $BaCO_3$ produced at the same experimental conditions ranged from 17.0 ± 0.01 and 17.4 ± 0.20‰ with a mean value of 17.2 ± 0.40‰.

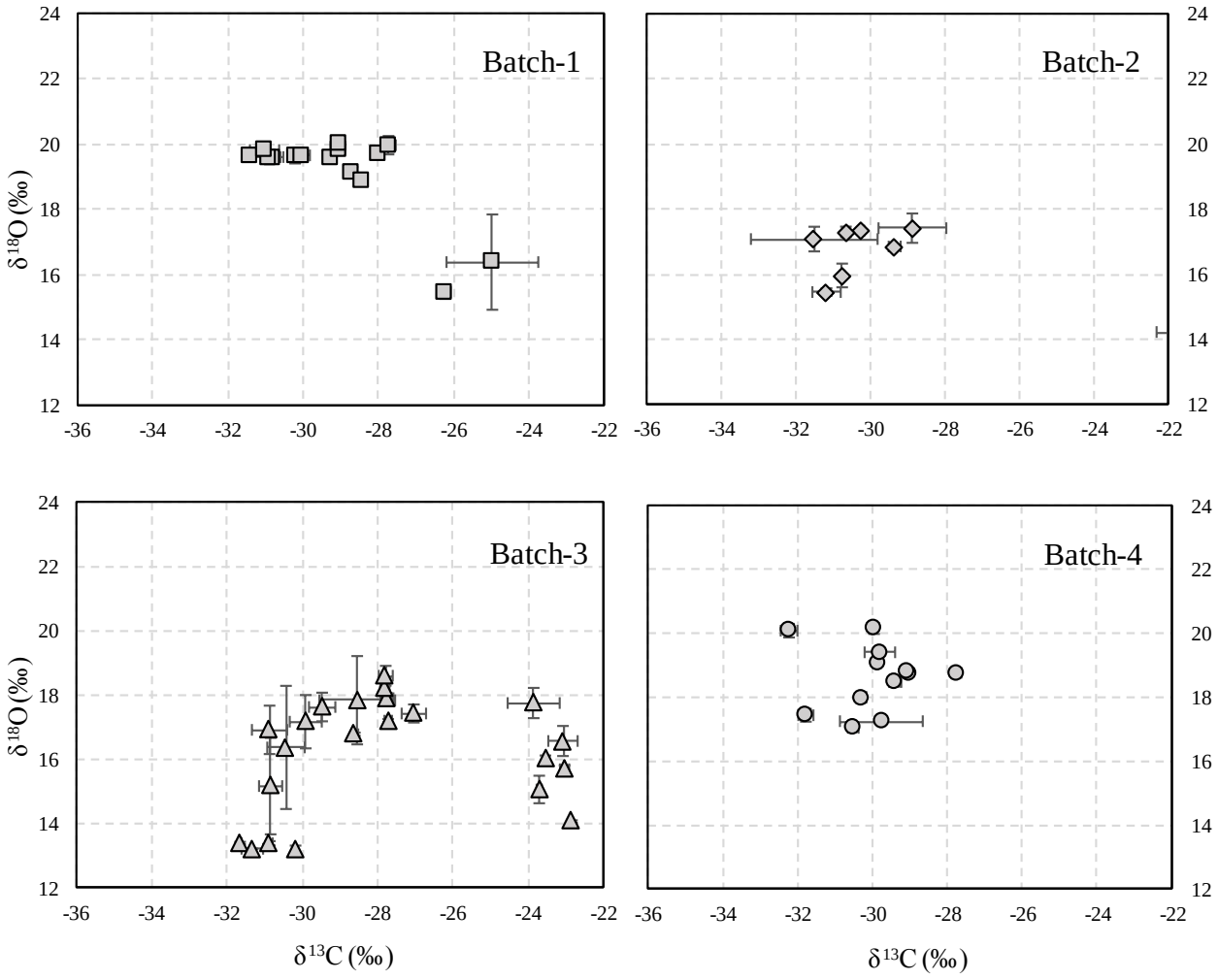

Figure 2.3. The $\delta^{13}C$ (vs. VPDB) and $\delta^{18}O$ (vs. VSMOW) values of all 4 batches. The temperature and pH of the experiments are discussed in detail in Section 4.2. Error-bars represent the 2σ standard deviations between a sample measurement and its replicate measurement for both $\delta^{13}C$ and $\delta^{18}O$ values (see Section 3.4 for details).

5. DISCUSSION

5.1 Potential Factors Influencing Isotopic Compositions of $BaCO_3$

The variation in $\delta^{13}C$ and $\delta^{18}O$ values of $BaCO_3$ samples produced at pH ≥ 9, pH ≤ 8.5 and at T=18°, 21°, 25°, and 30°C (Fig. 2.3; also see Table A1 in Appendix), suggests little to no systematic dependence to temperature and pH. The moles of Ba in the initial reactor solution for all experiments in each batch were greater than the moles of Ba calculated from the mass of the final $BaCO_3$ precipitates (see Appendix Table A2). On average, only ~11% from the initial moles of Ba were precipitated in the final $BaCO_3$. This suggests that HCO_3^-/CO_3^{2-} was quantitatively precipitated out of the reactor solution. The range in $\delta^{13}C$ and $\delta^{18}O$ values of $BaCO_3$ that is observed in the four batches may in part be due to experimental errors which include, temperature inconsistencies, invasion of $NaHCO_3$ stock solution inside the reactor chamber, and internal to external gas exchange due to improper seals at tube connections. In the forthcoming paragraphs, three potential experimental errors will be discussed to help validate the $\delta^{13}C$ and $\delta^{18}O$ values that best reflect the values we will use to determine KIEs in this study.

The first potential source of error is due to inconsistent temperature control, which affected Batch-1 and Batch-2 experiments. The temperature of the reactor chamber and stock solution vessel in Batch-1 and Batch-2 experiments were approximately the same as the ambient lab air which ranged between 20° and 24°C over the course of the experiment. Thus, without any control, experimental temperatures could fluctuate between 20° and 24°C throughout the duration of the experiment. This results in substantial uncertainty in our estimation of $\delta^{13}C$ and $\delta^{18}O$ values for equilibrium CO_2 and instantaneous HCO_3^- because the relevant fractionation factors ($^{13}\varepsilon/\alpha$ and $^{18}\varepsilon/\alpha$) required for the calculation of KIF are all sensitive to temperature (Table 2.3; See also Eq. (2.7), (2.10), (2.17), and (A2.1); Brenninkmeijer et al., 1983; Usdowski

and Hoefs, 1990; Zhang et al., 1995; Beck et al., 2005). Variations in $\delta^{13}C$ and $\delta^{18}O$ values for equilibrium $CO_{2\,(g)}$ and instantaneous HCO_3^- would affect the accuracy of the values calculated for ^{13}KIF and ^{18}KIF (see Eq. (2.8) and (2.12)). To minimize the issue for Batch-3 and Batch-4, we placed the stock solution chamber in a circulating water bath and insulated the reaction chamber.

The second potential source of error is $BaCO_3$ precipitation from direct interaction with the $NaHCO_3$ stock solution and the Tris-$BaCl_2$ reactor solution, rather than the reaction between $CO_{2\,(g)}$ and the reactor solution. During the equilibration of $CO_{2\,(g)}$ with the $NaHCO_3$ stock solution, internal gas was steadily pumped between the stock solution and reactor chamber (Section 3). In some experiments, droplets of $NaHCO_3$ stock solution were taken up into the gas flow of the experimental setup and transferred to the bottom of the reactor chamber due to vigorous bubbling in the stock solution. Over several hours, the droplets would accumulate in the reactor chamber, which was visible across the internal wall and over the fritted-disk located on the bottom of the reactor. Because the experimental system was to remain closed, there was no mechanism to remove the stock solution that entered the reactor chamber without compromising the equilibration process. Hence, the stock solution remained in the chamber during the precipitation of $BaCO_3$. To mitigate stock solution contamination, we attached a liquid/vapor trap to a tube connecting the stock solution vessel to the reactor chamber. The use of the liquid/vapor trap was fully implemented in batches 3 and 4. Although the trap reduced the amount of $NaHCO_3$ stock solution entering the reactor chamber, contamination still occurred sometimes which was evident by a light layer of mist that accumulated along the walls of the reactor chamber.

It was noted for two experimental runs, one from Batch-2 and one from Batch-3, that a large volume (estimated to be ~20mL) of stock solution entered the reactor chamber. The volume of stock solution was large enough to form bubbles above the frit prior to adding Tris-$BaCl_2$ reactor solution to precipitate $BaCO_3$. The $\delta^{13}C$ and $\delta^{18}O$ value of $BaCO_3$ produced from the Batch-2 experiment are -19.7 ± 3.76‰ and 14.2 ± 0.03‰, and the $\delta^{13}C$ and $\delta^{18}O$ value of $BaCO_3$ produced from the Batch-3 experiment are -23.7 ± 0.43‰ and 15.0 ± 0.07‰, respectively. The contaminated $BaCO_3$ sample from Batch-2 exhibited a 10.7‰ enrichment in ^{13}C when compared to the average $\delta^{13}C$ value of all other experiments in the same batch. Similarly, the contaminated $BaCO_3$ sample from Batch-3 was enriched in ^{13}C by 4.3‰ when compared to the average $\delta^{13}C$ value of all other Batch-3 experiments. Since the $NaHCO_3$ dissolved in the stock solution has a $\delta^{13}C$ value of -2.8 ± 0.08‰, which is substantially higher than the calculated $\delta^{13}C_{CO_2\,(g)}$ of about -11 to -10‰ (Table 2.3), then the ^{13}C enrichments in $\delta^{13}C$ of the two $BaCO_3$ samples mentioned may be due to the direct reaction with $NaHCO_3$ stock solution during $BaCO_3$ precipitation.

For oxygen, $NaHCO_3$ used in the stock solution had a $\delta^{18}O$ value of 14.6 ± 0.07‰ (vs. VSMOW). As the HCO_3^- in $NaHCO_3$ stock solution approaches isotopic equilibrium with H_2O, the $\delta^{18}O$ value of stock solution HCO_3^- will increase to ~27.8‰ at 25°C (calculated using $^{18}\varepsilon_{HCO_3^-\text{-}H_2O}$ from Beck et al. (2005) and the measured $\delta^{18}O_{H_2O}$ = -3.1 ± 0.08‰ (vs. VSMOW); See Eq. (A2) in the Appendix). $BaCO_3$ produced with stock solution contamination from Batch-2 was depleted in ^{18}O by 2.5‰ when compared to the average $\delta^{18}O$ value of Batch-2 experiments. The contaminated $BaCO_3$ sample from Batch-3 was depleted in ^{18}O by 1.2‰ when compared to the average $\delta^{18}O$ value of Batch-3 experiments.

The third experimental error considered is the possibility of gas exchange between external air and internal experimental gas during the equilibration period caused by an improper seal at a tube connection. If gas exchange between the internal gas and ambient lab air occurred there is a possibility that full isotopic equilibrium between $CO_{2\,(g)}$ and the stock solution would not be reached. As mentioned in an earlier section, if full isotopic equilibrium between $CO_{2\,(g)}$ and the stock solution is not established it would influence the $\delta^{13}C$ and $\delta^{18}O$ values of $BaCO_3$. There is also a possibility that isotopic equilibrium between $CO_{2\,(g)}$ and the stock solution was established however, the equilibrated $CO_{2\,(g)}$ would be a mixture of ambient lab air and $CO_{2\,(g)}$ produced from stock solution rather than evolving from the stock solution due to air entering and/or escaping the system. If this were the case, the equilibrium $CO_{2\,(g)}$ would have different $\delta^{13}C$ and $\delta^{18}O$ values than those calculated from equilibrium fractionation factors.

The isotopic composition of $CO_{2\,(g)}$ within the experimental system would reflect a mixture of CO_2 sources if there was contamination by ambient air ($CO_{2\,(g)}$). For carbon, there are three sources of $CO_{2\,(g)}$: 1) CO_2 evolved from the stock solution, 2) from human respiration, and 3) the local atmospheric CO_2. The concentration of $CO_{2\,(g)}$ produced from the stock solution is 1M or 35,500 ppm. Affek and Eiler (2006) measured the $\delta^{13}C$ (relative to VPDB) and $\delta^{18}O$ (relative to VSMOW) values of CO_2 from human respiration. However, since the $\delta^{18}O$ value will vary depending on location, only the $\delta^{13}C$ value will be considered from this study. The average $\delta^{13}C$ (n=7) value of respired $CO_{2\,(g)}$ was about -21.2 ± 0.02‰ with an average $CO_{2\,(g)}$ concentration of ~14,030 ppm (Affek and Eiler, 2006). The $\delta^{13}C$ value of atmospheric CO_2 measured at Mauna Loa, Hawaii in 2014 had a monthly mean value of -8.4 ± 0.07‰ and an annual mean concentration of CO_2 in 2018 of ~408 ppm (NOAA/ESRL, 2019). Additionally,

indoor CO_2 concentrations between 1000-1200 ppm is considered acceptable for indoor air quality according to the American National Standard Institute (AHSRAE, 2016). Because $CO_{2\,(g)}$ was not measured in our experimental setup we can only speculate on how CO_2 contamination would impact the $\delta^{13}C$ values of $BaCO_3$. If all of the $CO_{2\,(g)}$ inside of the experimental system was replaced with ambient $CO_{2\,(g)}$, then we could expect to see a decrease in $\delta^{13}C$ values of $BaCO_3$, because it is likely that respired $CO_{2\,(g)}$ makes up most of the ambient $CO_{2\,(g)}$, which is depleted in ^{13}C relative to both atmospheric $CO_{2\,(g)}$ and $CO_{2\,(g)}$ equilibrated with the stock solution. However, in order to successfully precipitate $BaCO_3$, the $CO_{2\,(g)}$ concentration in the system must exceed the $CO_{2\,(g)}$ concentration of the ambient lab space, which was proven by a failed experimental test where we attempted to precipitate $BaCO_3$ using only the $CO_{2\,(g)}$ in the ambient lab. Thus, it is likely that the majority of the $CO_{2\,(g)}$ within the experimental system evolved from the stock solution and that contamination of ambient $CO_{2\,(g)}$ would have a small effect on the $\delta^{13}C$ values of $BaCO_3$.

It is much more difficult to speculate how ambient air contamination affects the $\delta^{18}O$ values of $BaCO_3$ compared to $\delta^{13}C$ values because the $\delta^{18}O$ value of respired CO_2 depends on the $\delta^{18}O$ value of the local H_2O in the environment. According to Scholl et al. (2007), the $\delta^{18}O$ value of rainfall (i.e. source of the tap water in Hawaii) ranged between ~1 and 3‰. However, the measured oxygen isotope composition of H_2O used in the stock solution has a $\delta^{18}O$ value of -3.1‰. Since H_2O is the largest isotopic reservoir of oxygen and if we assume equilibrium between H_2O and $CO_{2\,(g)}$, then the contamination of ambient $CO_{2\,(g)}$ would have a small effect on the $\delta^{18}O$ values of $BaCO_3$. If oxygen isotope equilibrium is not established between $CO_{2\,(g)}$ and H_2O, then it is to be expected that the $\delta^{18}O$ value of $CO_{2\,(g)}$ would exhibit stronger ^{18}O

depletions relative to the $\delta^{18}O$ value of equilibrium $CO_{2\,(g)}$. In turn, the $\delta^{18}O$ values of $BaCO_3$ produced from $CO_{2\,(g)}$ out of equilibrium with the stock solution would likely exhibit lower values when compared to the $\delta^{18}O$ values of $BaCO_3$ produced from equilibrium $CO_{2\,(g)}$, however, this is not evident by the $\delta^{18}O$ values of $BaCO_3$.

Two additional techniques were employed during Batch-4 experiments to ensure there were no air leaks. The first technique was to test for leaks by attaching a hand pump to a tube which was connected to a valve. Before starting an experiment, an attempt was made to pump air through the tube. If the experimental set-up was not sufficiently sealed, the hand pump would be able to push air through. If the system was fully sealed, no air could be pushed through. The second technique used a syringe to insert the reactor solution into the reactor chamber. The procedure for inserting the reactor solution prior to implementing the new syringe technique was to open the valve, quickly insert the reactor solution, then close the valve. This method inevitably caused some of the internal gas of the experiment to escape while the valve was opened to introduce the reactor solution into the chamber. Hence, to limit gas exchange we applied the syringe technique, which was implemented as follows. First, the reactor solution was put in a syringe. Second, the syringe was sealed to a tube connected to a closed valve atop the reactor chamber a few minutes before the end of the equilibration period. Finally, when it was time to release the reactor solution into the chamber, the valve was opened and, without any exposure to ambient air, the reactor solution was inserted into the reactor chamber by the connected syringe. Since Batch-4 was the only one that utilized the two techniques described above, it is most likely that the $\delta^{13}C$ and $\delta^{18}O$ values of $BaCO_3$ were the least affected by air entering or leaving the system.

The discussion above suggest the $\delta^{13}C$ and $\delta^{18}O$ values of $BaCO_3$ from experiments in batches 1, 2, and 3 were likely the most affected by experimental errors. Some of the $\delta^{13}C$ and $\delta^{18}O$ values of $BaCO_3$ produced in batches 1, 2, and 3 may accurately reflect the results of an ideal experimental run, however, because of the errors associated with several of the experiments within those batches it is not certain which values are the most reliable. Batch-4 experiments were performed under the most ideal conditions where temperature was fully controlled, a vapor catch was used to limit invasion of $NaHCO_3$ stock solution, and several precautions were made to ensure the experimental system was fully sealed before every experimental run. Because all of Batch-4 $BaCO_3$ samples were produced under optimized experimental conditions and likely represent the most accurate $\delta^{13}C$ and $\delta^{18}O$ values to reflect CO_2 hydration, only Batch-4 results will be used to calculate KIEs in the forthcoming paragraphs.

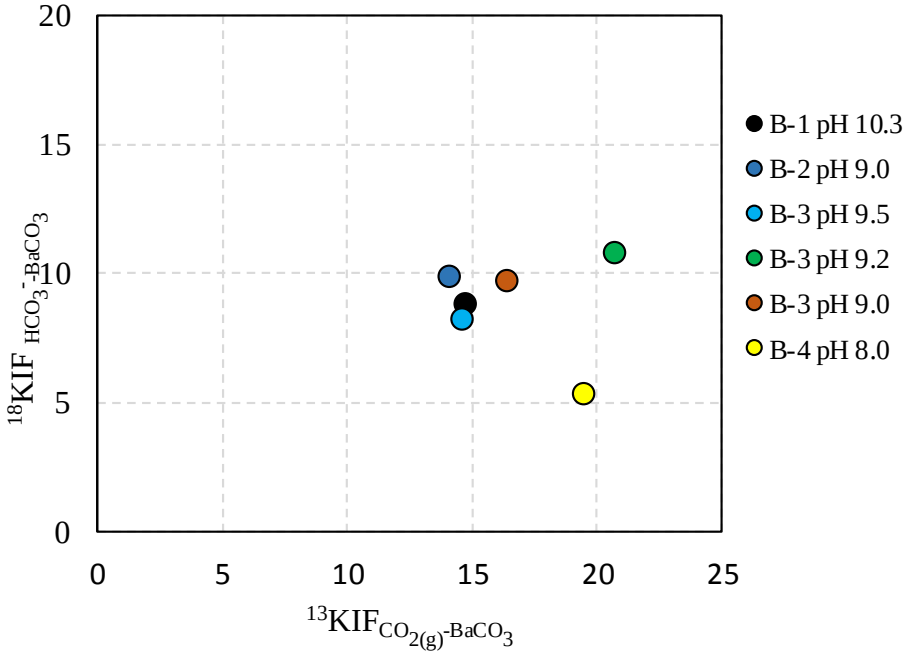

Fig. 2.4. The average $^{13}KIFs$ and $^{18}KIFs$ at pH ≥ 9.0 from batches 1, 2, and 3 compared to the average ^{13}KIF and ^{18}KIF of Batch-4 data at pH 8.0. Each color represents the pH at which each experiment was conducted.

5.2 KIF During CO_2 Hydration

Apparent carbon and oxygen isotope fractionation as a result of KIEs for CO_2 hydration can be quantified by comparing $\delta^{13}C$ and $\delta^{18}O$ values of the $BaCO_3$ samples to $\delta^{13}C$ of $CO_{2\,(g)}$ (Eq. (2.8)) and $\delta^{18}O$ of instantaneously formed HCO_3^- (Eq. (2.12)), respectively, that are constrained for the equilibrium condition (Fig. 2.2). The calculated experimental KIFs represent the magnitude of the isotope fractionation, such that they are reported as positive values. Based on the justification of results provided in Section 5.1 only Batch-4 data will be discussed for the remainder of this section, with the exception of Section 5.2.1 where the effects of pH will be briefly considered. Furthermore, for the remainder of this paper, Batch-4 KIFs will be reported as $^{13}KIF_{Batch\text{-}4}$ and $^{18}KIF_{Batch\text{-}4}$ for carbon and oxygen, respectively, and are defined by the values reported in Table 2.4.

The absolute uncertainty for individual KIFs is reported as the error propagation using the $\pm 2\sigma$ S.D. of the relevant equilibrium fractionation factors and the $\pm 2\sigma$ S.D. of the average $\delta^{13}C$ and $\delta^{18}O$ values of each sample and its duplicate measurement. The absolute uncertainty for mean KIFs is the $\pm\ 2\sigma_m$ calculated from the error propagated from the analytical uncertainty between each sample and its replicate and the propagated uncertainty of the derived equilibrium ^{13}C and $\delta^{18}O$ values. The $^{13}KIF_{Batch\text{-}4}$ calculated between $CO_{2\,(g)}$ and $BaCO_3$ at T=25°C and pH 8.0 range from 17.6 ± 0.29 to 22.2 ± 0.39‰ with a mean value ($\pm 2\sigma_m$; n=10) of 19.6 ± 0.12‰ (Table 2.4). The calculated $^{18}KIF_{Batch\text{-}4}$ between HCO_3^- instantaneously produced from CO_2+H_2O range from 4.0 ± 0.19 to 6.9 ± 0.33‰ with a mean value ($\pm 2\sigma_m$; n=10) of 5.3 ± 0.09‰ (Table 2.4). Mean KIFs calculated for all batches are provided in Table A3 in the Appendix.

5.2.1 Effects of CO_2 Hydroxylation

As pH increases above pH 9, the CO_2 hydration reaction becomes less favorable and CO_2 hydroxylation becomes dominant (as mentioned in Section 2; Kern, 1960). Additionally, there is some evidence to support the KIFs associated with the reactions from Eq. (2.5) and (2.6) differ (Siegenthaler and Münnich, 1981; Marlier and O'Leary, 1984; Clark et al., 1992). The mean $^{13}KIF_{CO_{2\,(g)}\text{-}BaCO_3}$ and $^{18}KIF_{HCO_3^-\,(instant)\text{-}BaCO_3}$ (n=11) at pH ≥ 9 is 16.3 ± 2.60 and 9.6 ± 0.74‰ (σ_m). When the average ^{13}KIF and ^{18}KIF from high pH experiments is compared to the average $^{13}KIF_{Batch\text{-}4}$ and $^{18}KIF_{Batch\text{-}4}$ at pH 8.0 (mean $^{13}KIF_{Batch\text{-}4} = 19.6 \pm 0.25$‰ and $^{18}KIF_{Batch\text{-}4} = 5.3 \pm 0.55$‰) there is a~ -3.3 and +4.3‰ difference, respectively. If there was a systematic trend observed for carbon and oxygen, one might expect the change in both ^{13}KIF and ^{18}KIF with increasing pH to be consistent. Instead, the ^{13}KIF and ^{18}KIF vary independently where ^{13}KIF decreases and ^{18}KIF increases with increasing pH (Fig. 2.4). Given these results, we refrain from providing a robust statement on KIFs during CO_2 hydroxylation.

Table 2.4. Batch-4 ^{13}KIF between equilibrium $CO_{2(g)}$ and experimental $BaCO_3$ and ^{18}KIF between instantaneous HCO_3^- and experimental $BaCO_3$, calculated from Eq. (15) and (16), respectively. The mean ^{13}KIF and ^{18}KIF at T=25°C is also reported. All Batch-4 experiments were conducted at pH 8.0. The uncertainty for the calculated KIFs represents a 2σ standard deviation. The mean uncertainties represent the 95% confidence interval of the standard deviation of the mean ($2\sigma_m$) for Batch-4 samples at T=25°C.

Batch-4 Sample #	T (°C)	$^{13}KIF_{CO_2\ (g)-BaCO_3}$	$^{18}KIF_{HCO_3^-(instant)-BaCO_3}$
B4-1	18	19.6 ± 0.31	7.8 ± 0.35
B4-2	18	21.0 ± 0.35	6.3 ± 0.29
B4-3	25	19.9 ± 0.33	4.0 ± 0.19
B4-4	25	17.6 ± 0.29	5.4 ± 0.25
B4-5	25	19.5 ± 0.79	6.9 ± 0.33
B4-6	25	18.9 ± 0.31	5.4 ± 0.24
B4-7	25	19.0 ± 0.31	5.3 ± 0.24
B4-8	25	20.2 ± 0.33	6.2 ± 0.28
B4-9	25	22.3 ± 0.39	4.1 ± 0.19
B4-10	25	19.8 ± 0.32	5.1 ± 0.23
B4-11	25	19.2 ± 0.33	5.7 ± 0.28
B4-12	25	19.6 ± 0.42	4.8 ± 0.23
Mean	25	19.6 ± 0.23	5.3 ± 0.28
Mean*	25	17.6 ± 0.43*	--

*The mean ^{13}KIF value of Batch-4 including the ^{13}KIF between $CO_{2(g)}$ and $CO_{2(aq)}$ determined by Mook (1986) and others to be ~2‰.

5.2.2 Isotope Fractionation Between $CO_{2\ (g)}$ and $CO_{2\ (aq)}$

The mean $^{13}KIF_{Batch\text{-}4}$ calculated from the values listed in Table 2.4 is 19.6 ± 0.25‰, which assumes that HCO_3^- was produced from $CO_{2\ (aq)}$ that had a $\delta^{13}C$ value equal to the $\delta^{13}C$ value calculated for $CO_{2\ (g)}$ (Table 2.3). However, the very first step for the interactions between the $CO_{2\ (g)}$ and reactor solution is the diffusion across the gas-liquid interface provided by the bubbling (see Fig. 2.1b):

$$CO_{2\ (g)} \leftrightarrow CO_{2\ (aq)} \qquad (2.16)$$

Thus, it is the dissolved $CO_{2\,(aq)}$ that reacts with H_2O to yield HCO_3^-. The equilibrium $^{13}\varepsilon$ associated with Eq. (2.16) was previously constrained by Zhang et al. (1995):

$$^{13}\varepsilon_{CO_{2\,(aq)}\text{-}CO_{2(g)}} = -(0.0049 \pm 0.003)(T) - 1.31 \pm 0.06‰ \quad (2.17)$$

where T is temperature in °C and $^{13}\varepsilon_{CO_{2\,(aq)}\text{-}CO_{2(g)}}$ =1.4‰, where $CO_{2\,(aq)}$ is depleted in ^{13}C by 1.4‰ relative to equilibrium $CO_{2\,(g)}$ at T=25°C. So, the values for $^{13}KIF_{Batch\text{-}4}$ in Table 2.4 would decrease by 1.4‰ and the mean $^{13}KIF_{Batch\text{-}4}$ would equal 18.2‰. Other values constrained for $^{13}\varepsilon_{CO_{2\,(aq)}\text{-}CO_{2(g)}}$ by other authors agree well with Zhang et al. (1995), with a standard deviation of 0.2‰ (Vogel et al., 1970; Zhang et al., 1995; Szaran, 1998).

In the case where the reaction from Eq. (2.16) does not reach equilibrium, there is a ^{13}KIE to be considered. Previous experimental studies to determine $^{13}KIEs$ associated with Eq. (2.16) reported a $^{13}KIF_{CO_{2(g)}\text{-}CO_{2(aq)}}$ of ~2.0 ± 0.20‰ at 25°C, where $CO_{2\,(aq)}$ is depleted in ^{13}C relative to $CO_{2\,(g)}$ (Inoue and Sugimura, 1985; Wanninkof, 1985; Mook, 1986; Zhang et al., 1995). In this study, we assume full ^{13}KIF between $CO_{2\,(g)}$ and $CO_{2\,(aq)}$, so the values reported in Table 2.4 would be lower by ~2.0 ± 0.20‰ and the mean $^{13}KIF_{Batch\text{-}4}$ should be ~17.6 ± 0.23‰ .

For oxygen, Vogel et al. (1970) reported the $^{18}\varepsilon_{CO_{2(aq)}\text{-}CO_{2\,(g)}}$ to be 0.8‰ at 0°C where $CO_{2\,(aq)}$ is enriched in ^{18}O relative to $CO_{2\,(g)}$. Due to gas sampling limitations, higher temperature values for $^{18}\varepsilon_{CO_{2(aq)}\text{-}CO_{2\,(g)}}$ were deemed unreliable (Vogel et al., 1970). To the best of our knowledge, Vogel et al. (1970) is the only study that attempted to constrain $^{18}\varepsilon_{CO_{2(aq)}\text{-}CO_{2\,(g)}}$ and we are unaware of a study that determined ^{18}KIF between $CO_{2\,(g)}$ and $CO_{2\,(aq)}$.

5.3 Previous Experimental and Theoretical Studies

Previous experimental ^{13}KIFs reported during CO_2 hydration (see Table 2.1) were inconsistent amongst studies and ranged widely between 6.9 and 19.7‰ (Marlier and O'Leary, 1984; Clark and Lauriol, 1992; O'Leary et al., 1992; Sade and Halevy, 2017; 2019). The average $^{13}KIF_{CO_2-HCO_3^-}$ determined from Clark and Lauriol's (1992) experimental results agrees best with our average $^{13}KIF_{Batch\text{-}4}$, differing by ~0.1‰. Although the average $^{13}KIF_{CO_2-HCO_3^-}$ from Clark and Lauriol's (1992) study was based on experiments conducted at 0°C, Zeebe (2014) calculated that the temperature dependence of ^{13}KIF during CO_2 hydration is at most 1.8‰ between 0° and 25°C. The smaller discrepancy between our $^{13}KIF_{Batch\text{-}4}$ at T=25°C and the ^{13}KIF reported by Clark and Lauriol at T=0°C compared to the temperature dependence calculated by Zeebe (2014) may suggest ^{13}KIFs are even less affected by temperature than what was previously estimated. The largest discrepancy of ~12.7‰ is observed between the average $^{13}KIF_{Batch\text{-}4}$ and the $^{13}KIF_{CO_2-HCO_3^-}$ reported by Marlier and O'Leary (1984), with the smaller ^{13}KIF reported by the latter. In comparison to Zeebe's (2014) theoretical calculations, our average $^{13}KIF_{Batch\text{-}4}$ compares best with the reported range of ~23 to 33‰, which are the values reported for the CO_2 hydration reaction mechanism involving $n \geq 4$ water molecules (Table 3 in Zeebe (2014)). The lower ^{13}KIF value in the range reported by Zeebe for n=4 and n=8 water molecules is ~3.4‰ larger than our mean $^{13}KIF_{Batch\text{-}4}$ of 19.6 ± 0.12‰. In contrast, a discrepancy of ~9.5‰ and 5.5‰ is observed between the mean $^{13}KIF_{Batch\text{-}4}$ and the values for ^{13}KIF reported for n=1 and n=3 water molecules, respectively. The 5.5‰ increase in the ^{13}KIF reported for n=3 water molecules to the value we report as the mean $^{13}KIF_{Batch\text{-}4}$ may be indicative of the reaction mechanism switching from a one-step hydration mechanism to a multi-step hydration mechanism involving $n \geq 4$, first recognized in the initial reporting by Zeebe (2014) when the

theoretical ^{13}KIFs reported increased by 6.5‰ as n increased from 3 to 4 water molecules. If the larger $^{13}KIF_{Batch\text{-}4}$ compared to the ^{13}KIF reported for $n \geq 4$ indicates a multi-step hydration mechanism, then the dominant reaction pathway for the CO_2 hydration reaction is to proceed stepwise through a HCO_3^--H_3O^+ intermediate state (see Eq. (2.4) where the reaction proceeds via I→II→III), rather than a concerted pathway to lead directly to the products (i.e. I→III, see Eq. (2.4)).

The average $^{18}KIF_{Batch\text{-}4}$ calculated from Table 2.4 is 5.3± 0.09‰ at 25°C and pH 8.0. However, to directly compare the ^{18}KIFs of this study to those reported in previous studies we will define the mean ^{18}KIF to be between equilibrium $CO_{2\ (g)}$ and Batch-4 $BaCO_3$ (written here as, $^{18}KIF_{Batch\text{-}4*}$), which has a mean value of 18.7 ± 0.02‰. The only available experimental data for ^{18}KIF is reported by Clark and Lauriol (1992), who determined the ^{18}KIF for HCO_3^- dehydration. Based on the relationship between equilibrium fractionation and KIF described by Eq. (2.3) and by the value reported by Sade and Halevy (2017; 2018), the ^{18}KIF based on the experimental data of Clark and Lauriol (1992) yields a ^{18}KIF for the CO_2 hydration of ~3.7‰, which is ~15‰ smaller than our average $^{18}KIF_{Batch\text{-}4*}$. As mentioned in Section 1.1, one of the issues with the study by Clark and Lauriol (1992), was that the cryogenically produced $CaCO_3$ runs the risk of producing mixed polymorphs (i.e. carbonate precipitation other than calcite), which can affect KIFs. Because of the uncertainty in the ^{18}KIF reported by Clark and Lauriol (1992), Sade and Halevy (2017;2019) assumed calcite as the only polymorph and re-calculated their ^{18}KIF during CO_2 hydration to be 7.3‰, which is ~11‰ smaller than our average $^{18}KIF_{Batch\text{-}4*}$. Sade and Halevy (2017; 2019) also re-calculated ^{18}KIFs reported originally in the theoretical studies by Zeebe (2014) and Guo (2008) as described in Section 1.1. The calculated ^{18}KIF for CO_2 hydration based on the results of Guo (2008) was estimated to be 16.4‰ (Sade

and Halevy 2017; 2018). More recently, Guo and Zhou (2019) reported theoretical estimates of ^{18}KIF for CO_2 hydration to be 4.3 and 8.7‰ where the difference between the two values is the result of ^{18}O coming from CO_2 or H_2O, respectively at 25°C. Guo and Zhou (2019) reported 4.3‰ for ^{18}KIE during CO_2 hydration, which is ~14‰ smaller than the mean $^{18}KIF_{Batch\text{-}4*}$. The range for ^{18}KIFs reported by Zeebe (2014) is 13-15‰ for $n \geq 4$ water molecules and between ~11-15‰ for $n \leq 3$ water molecules, where the larger value in both ranges agree best with our average $^{18}KIF_{Batch\text{-}4*}$ compared to all other experimental and theoretical estimates mentioned for ^{18}KIF. It is stated in Zeebe (2014) that the ^{18}KIF during CO_2 hydration is likely to be smaller than that of carbon for $n \geq 4$ because rate constants for ^{18}KIF and oxygen isotope fractionation without subsequent oxygen exchange are similar in magnitude, which suggests the total oxygen KIF will be less affected by ^{18}O and ^{16}O isotope exchange.

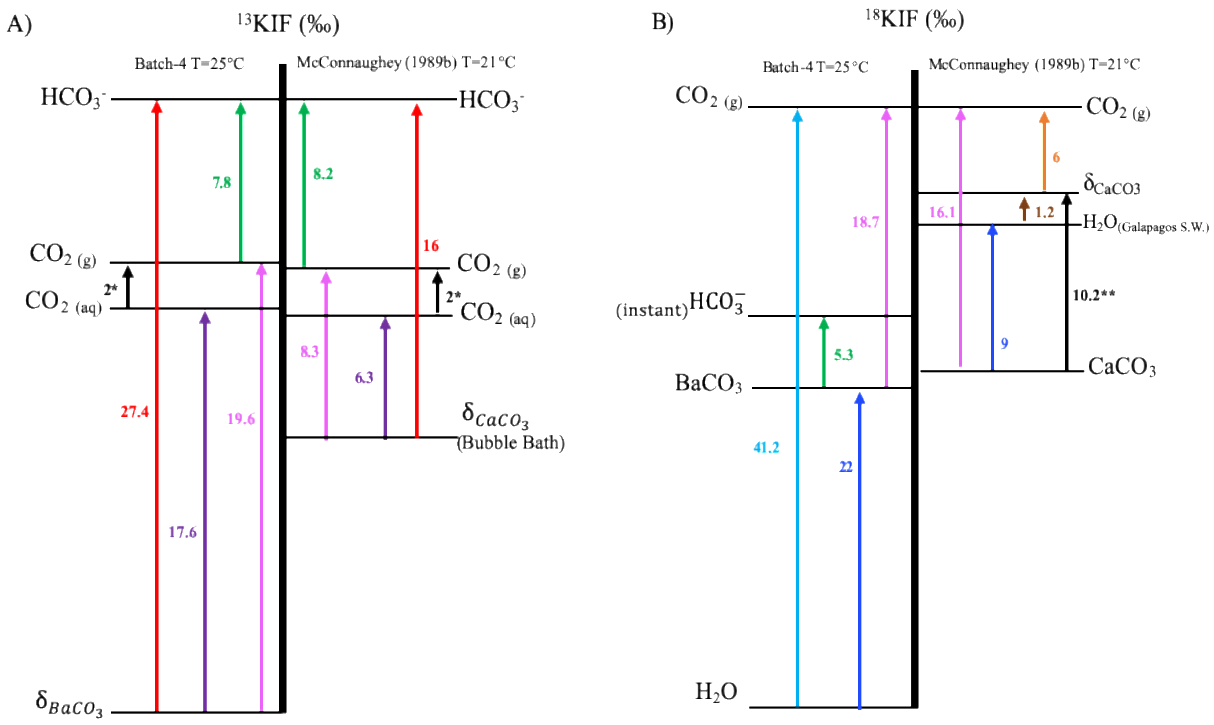

Fig. 2.5. A schematic illustration comparing mean ^{13}KIFs and ^{18}KIFs from Batch-4 and McConnaughey (1989) at T=25°C and 21°C, respectively, where the scaling of the arrows denoting KIFs is only estimated. **A)** The ^{13}KIFs of Batch-4 (left of center axis) and McConnaughey (right of center axis) in permil (‰). The ^{13}KIF between $BaCO_3$/ $CaCO_3$ and equilibrium HCO_3^- (red arrows) were calculated from the $\delta^{13}C$ of $BaCO_3$/ $CaCO_3$ and the measured $\delta^{13}C$ value of $NaHCO_3$ for Batch-4, and the known $^{13}\varepsilon_{HCO_3^- - CO_2}$ reported by Emrich et al. (1970) and Deines et al. (1974) for McConnaughey (green arrow). The ^{13}KIF between $BaCO_3$/ $CaCO_3$ and $CO_{2\ (aq)}$ (purple arrows; *i.e. 2‰ less than if compared to $CO_{2\ (g)}$ (magenta arrows; Mook, 1986)), where $CO_{2\ (g)}$ of Batch-4 was derived from Eq. (2.7) and the measured $\delta^{13}C$ value of $NaHCO_3$, and the $CO_{2\ (g)}$ from McConnaughey was directly measured. The ^{13}KIF between $CO_{2\ (g)}$ and $CO_{2\ (aq)}$ (Eq. (2.17)) and the $\delta^{13}C$ values for $CO_{2\ (g)}$ from Batch-4 and McConnaughey were used to calculate the final ^{13}KIF between $BaCO_3$/ $CaCO_3$ and $CO_{2\ (aq)}$. **B)** The ^{18}KIFs of Batch-4 (left of axis) and McConnaughey (1989) (right of axis). The line labelled δ_{CaCO_3} on the right side of the center axis represents the $\delta^{18}O$ value of $CO_{2\ (g)}$ liberated from $CaCO_3$ by acid dissolution in equilibrium with VSMOW. **The acid fractionation factor between the liberated $CO_{2\ (g)}$ and the solid $CaCO_3$ is ~10.2‰, so the true $\delta^{18}O$ value of McConnaughey's solid $CaCO_3$ is ~10.2‰ lighter than δ_{CaCO_3} (black arrow), which will be the value used to calculate ^{18}KIFs that can be directly compared to ^{18}KIFs of Batch-4. The ^{18}KIF between $BaCO_3$ and $CO_{2\ (g)}$ (magenta arrow) was determined from the $\delta^{18}O$ value of $CO_{2\ (g)}$ derived from the relationship between Eq. (2.10) ($^{18}\varepsilon_{CO_{2\ (g)}-H_2O}$; light blue arrow) and the measured $\delta^{18}O$ value of H_2O (-3.1‰). The same ^{18}KIF for McConnaughey was calculated using the measured $\delta^{18}O$ value of $CO_{2\ (g)}$ used in the experiments. The ^{18}KIF we defined from Eq. (2.12) is given by the green arrow.

5.3.1 Comparison to KIF of McConnaughey (1989)

McConnaughey (1989) reported ^{13}KIEs of his experimental results relative to two equilibrium δ^{13}C values. The first ^{13}KIF was calculated by comparing the measured δ^{13}C of the CO_2 source gas to the δ^{13}C of his experimental $CaCO_3$ ($^{13}KIF_{CO_{2(g)}-CaCO_3}$), which yielded an average $^{13}KIF_{CO_{2(g)}-CaCO_3}$ of 8.3‰ at 21°C and pH between 7.89 and 8.24. The second ^{13}KIF was calculated between experimental $CaCO_3$ and the δ^{13}C value expected for $CO_{2\,(g)}$ in isotopic equilibrium with Galapagos seawater at 21°C, which yielded an average $^{13}KIF_{Galapagos\ CO_2-CaCO_3}$ of ~16‰. To directly compare our results to McConnaughey, the former $^{13}KIF_{CO_{2(gO-CaCO_3}}$ will be used. There is a large discrepancy of ~11.3‰ between the mean $^{13}KIF_{Batch\text{-}4}$ and McConnaughey's mean $^{13}KIF_{CO_{2(g)}-CaCO_3}$ at T=25° and 21°C (Fig. 2.5 and Fig. 2.6).

McConnaughey (1989) defined ^{18}KIFs as the observed ^{18}O depletion in the experimental $CaCO_3$ relative to the measured $CO_{2\,(g)}$ source, which is associated with a ~10‰ enrichment in the δ^{18}O values. After accounting for the 10‰ enrichment, the ^{18}KIFs ranged from 15.9 to 16.3‰ at T = 21°C (n=2, $^{18}KIF_{average(T=21°C)}$ = 16.1‰) and 14.6 to 16.2‰ at T = 1.1 to 4.3°C (n=4, $^{18}KIF_{average(T<4°C)}$ = 15.4‰) (Fig. 2.5). When comparing the mean $^{18}KIF_{Batch-4*}$ at T=25°C to McConnaughey's $^{18}KIF_{CO_{2(g)}-CaCO_3}$ at 21°C, the difference is ~3‰, where Batch-4 $BaCO_3$ exhibits a stronger ^{18}O depletion relative to $CO_{2\,(g)}$ compared to the ^{18}O depletion observed in McConnaughey's $CaCO_3$ relative to $CO_{2\,(g)}$ (Fig. 2.5 and Fig. 2.6).

The close agreement observed between $^{18}KIF_{Batch-4*}$ and the $^{18}KIF_{CO_{2(g)}-CaCO_3}$ compared to the large difference between $^{13}KIF_{Batch-4*}$ and $^{13}KIF_{CO_{2(g)}-CaCO_3}$ might suggest re-equilibration between HCO_3^- and the reactants is being expressed in the ^{13}KIF of

McConnaughey's experimental $CaCO_3$. In contrast, because oxygen isotope equilibrium is slower than that of carbon isotopes, McConnaughey's ^{18}KIFs may be close to the full kinetic effect as full isotope dis-equilibrium is approached, which would hence explain the similarity in magnitude to the mean $^{18}KIF_{Batch-4*}$.

It is important to note that McConnaughey's $CO_{2\ (g)}$ source was analyzed for its carbon and oxygen isotopes, while the $\delta^{13}C$ and $\delta^{18}O$ of our $CO_{2\ (g)}$ was estimated from the relationship between the known $^{13}\varepsilon_{HCO_3^-\text{-}CO_{2(g)}}$ (Eq. (2.7)) and the measured $\delta^{13}C$ and $\delta^{18}O$ value of $NaHCO_3$. Unfortunately, McConnaughey (1989) did not provide enough information to confidently determine whether the $CaCO_3$ precipitation was truly quantitative. Also, the reaction time for $CaCO_3$ precipitation was not provided so it is unclear whether partial HCO_3^- re-equilibration with dissolved CO_2 could occur. If re-equilibration did occur, it is estimated that McConnaughey's ^{13}KIF values would approach $^{13}\varepsilon_{HCO_3^-\text{-}CO_{2(g)}}$, which is ~8.4‰ at T=21°C (Eq. (2.7); Zhang et al., 1995).

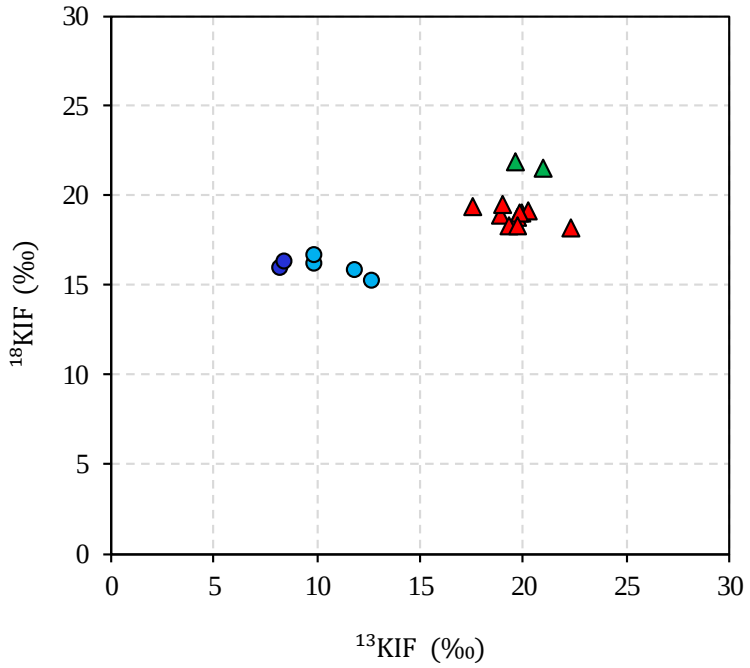

Fig. 2.6. A comparison between ^{13}KIFs and ^{18}KIFs of Batch-4 between $CO_{2\,(g)}$ and $BaCO_3$ at T = 18°C (green triangles) and 25°C (red circles), and the ^{13}KIFs and ^{18}KIFs between $CO_{2\,(g)}$ and $CaCO_3$ reported by McConnaughey (1989) at T = 21°C (dark blue circles) and 1.1 to 4.3°C (light blue circles). The positive increase in ^{13}KIFs and ^{18}KIFs indicates stronger ^{13}C and ^{18}O depletions in $BaCO_3$ (or $CaCO_3$) relative to equilibrium $CO_{2\,(g)}$.

6. CONCLUSIONS AND IMPLICATIONS

We performed quantitative $BaCO_3$ precipitation experiments to determine ^{13}KIF and ^{18}KIF during the hydration of CO_2. In all experiments performed in this study we observed kinetic effects on HCO_3^- during CO_2 hydration when the $\delta^{13}C$ and $\delta^{18}O$ values of $BaCO_3$ were compared to the $\delta^{13}C$ and $\delta^{18}O$ values derived for equilibrium $CO_{2\,(g)}$ and instantaneously formed HCO_3^-. However, experimental errors that occurred in the early stages of the project (i.e. Batches 1, 2 and 3) suggest that some experimental results are unreliable. The KIFs determined from Batch-4 data appear most reliable as those experiments were performed under most optimized conditions to minimize experimental errors. Based on these data we conclude the most

reliable ^{13}KIF and ^{18}KIF reported in this study is 19.6 ± 0.75‰ and 5.3 ± 0.55‰, which represent the mean ^{13}KIF and ^{18}KIF of Batch-4 experiments.

When compared to ^{13}KIFs reported previously for the hydration of CO_2, our mean experimental ^{13}KIF ($^{13}KIF_{Batch\text{-}4}$ = 19.6 ± 0.75‰) agrees best with the experimental ^{13}KIF from Clark and Lauriol (1992; ^{13}KIF = 19.7‰) and the theoretical ^{13}KIF calculated by Zeebe (2014; ^{13}KIF = 23 to 33‰ for n ≥ 4). The small discrepancy (~0.1‰) between the ^{13}KIF of Batch-4 and the value reported by Clark and Lauriol (1992), may suggest there is a very little temperature effect on KIEs during CO_2 hydration. For oxygen, our mean experimental ^{18}KIF between $CO_{2\,(g)}$ and $BaCO_3$ ($^{18}KIF_{Batch\text{-}4}$=18.9 ± 0.56‰) is ~2.8‰ larger than the largest experimental ^{18}KIF reported by McConnaughey (1989; Table 2.1) and ~4‰ larger than the largest ^{18}KIF calculated by Zeebe (2014).

Other than the single experimental study by Clark and Lauriol (1992), we report the largest ^{13}KIF and ^{18}KIF when compared to all of the experimental studies listed in Table 2.1. Our values being the largest might suggest our Batch-4 KIFs reflect full isotope disequilibrium during CO_2 hydration (or closest to full isotope disequilibrium), which would mean our values exhibit the full magnitude of the kinetic effect. From the comparison made between Batch-4 and the values reported by Zeebe (2014), our ^{13}KIF and ^{18}KIF compare best with the values Zeebe reported for the CO_2 hydration reaction mechanism involving n≥4 water molecules. If this is indeed the case, then it would suggest the dominant hydration pathway proceeds stepwise through a HCO_3^- - H_3O^+ intermediate state (i.e. I→II→III, see Eq. (2.3)).

Since Batch-4 experiments were only performed at T=25°C (n=10) and 18°C (n=2), it is unclear how variation in temperature below 18°C and above 25°C in these experiments would affect the magnitude of the ^{18}KIEs. Based on the similar ^{13}KIFs reported for Batch-4 and

Clark and Lauriol (1992) produced at 25° and 0°C, respectively, temperature appears to have little effect on the magnitude of the ^{13}KIE. For pH, Batch-4 $BaCO_3$ were produced from one reactor solution of pH 8.0, which is close to that of sea water pH (8.2). Variation observed in the $\delta^{13}C$ and $\delta^{18}O$ values of $BaCO_3$ produced at pH $\geq$ 9, pH $\leq$ 8.5 and at T=18°, 21°, 25°, and 30°C (Fig. 2.3), suggests little to no systematic dependence to the parameters manipulated in the experiments. However, the possible experimental errors associated with the batches containing these data make them less reliable so, additional tests to verify/falsify the effects of varying temperature and pH on KIEs would be necessary.

KIEs associated with the hydration of CO_2 is fundamental parameter that will be relevant to a wide range of studies. To the best of our knowledge, the results of this study represent the most systematic experimental study, which will help improve paleo-proxies interpretations since kinetic effects are present in biogenic carbonates used in paleoclimate reconstructions. Additionally, the results of this study will assist in resolving the molecular mechanism of the CO_2 hydration pathway, which has been a topic of theoretical studies for several years (e.g. Tautermann et al., 2002; Nguyen et al., 2008; Stirling and Papai, 2010; Wang and Cao, 2013; Zeebe, 2014). Determining the dominant pathway for the CO_2 hydration reaction is important because CO_2 hydration and its products play a large role in aqueous environments, which includes ocean acidification, biological carbon fixation, biological mineral precipitation, and more. Thus, understanding the underlying mechanism involved with the CO_2 hydration reaction can help re-evaluate KIEs involved in those various oceanic processes as well as provide insight into exactly how the ocean will respond to increasing atmospheric CO_2 concentrations.

CHAPTER 3. SUMMARY

The CO_2 hydration reaction is a fundamental chemical transformation, ubiquitous in aqueous solutions that contain DIC and critical in several geochemical, physicochemical, and biological processes. A characteristic KIE is associated with the CO_2 hydration reaction where the reaction product, HCO_3^-, is depleted in the heavy isotopes of carbon and oxygen. Prior to this study, the magnitude of KIEs during CO_2 hydration was not well constrained, evidenced by the sparse and inconsistent experimental data currently reported in the literature. We performed systematic precipitation experiments to report the most reliable KIF during CO_2 hydration.

To carry out the precipitation experiments we used an experimental approach that was modified from the methods described by McConnaughey (1989). Experimental errors in the early stages of the project were made apparent by the large variation in the carbon and oxygen isotope compositions measured in the first three batches of experimentally produced $BaCO_3$. Batch-4 experiments were performed under the most optimal experimental conditions and the more consistent results of the stable isotope analyses suggest Batch-4 data was the most reliable out of all four batches.

Our mean ^{13}KIF compared best with the ^{13}KIF reported by Clark and Lauriol (1992) at 0°C, which may suggest temperature has a small effect on this KIF. On the other hand, our mean ^{13}KIF and ^{18}KIF of 19.6 $\pm$ 0.75‰ and 18.7 $\pm$ 0.56‰, respectively, were the largest values of all of the experimental KIFs reported previously, which may suggest that our KIFs reflect the magnitude of the kinetic effect closest to full isotope disequilibrium during CO_2 hydration.

In the future, it would be beneficial to expand the experimental parameters tested in this study to include, for example, a larger temperature range. Additional experiments may also be done to account for possible systematic variations during $CaCO_3$ precipitation that are less

known due to the long time frame that is necessary for DIC species to fully equilibrate in solution (see Zeebe, 1999 and Watkins et al., 2013). To account for these possible systematic variations during $CaCO_3$ precipitation, the addition of the enzyme carbonic anhydrase (CA) could be used in future experiments to speed up equilibration between CO_2 and HCO_3^-, which would ensure no disequilibrium exists in solution (Uchikawa and Zeebe, 2012). These equilibrium precipitation experiments could then be compared with the results of our kinetic precipitation experiments to guarantee our KIFs are truly kinetically driven. Finally, future work to analyze the clumped isotope composition of our $BaCO_3$ samples would provide experimental results to aid in understanding isotope disequilibrium effects in isotope clumping during CO_2 hydration (Tripati et al., 2015; Daëron et al., 2019; Guo and Zhou, 2019).

APPENDIX

The inverse time constant $\frac{1}{\tau}$ to calculate the time it takes for oxygen isotopes to fully equilibrate (Zeebe and Wolf-Gladrow, 2001):

$$\tau^{-1} = (0.5) \cdot \{k_{+2} + k_{+4}[\mathrm{OH}^-]\} \cdot \left\{1 + \frac{[\mathrm{CO_2}]}{S} - \left[1 + \left(\frac{2}{3} \cdot \frac{[\mathrm{CO_2}]}{S}\right) + \left(\frac{[\mathrm{CO_2}]}{S}\right)^2\right]^{1/2}\right\} \quad \text{(A1-a)}$$

where, $[\mathrm{OH}^-]$ can be constrained from pH and known kinetic rate constants (Usdowski et al., 1991), and $S = [\mathrm{H_2CO_3}] + [\mathrm{HCO_3^-}] + [\mathrm{CO_3^{2-}}]$. The time required for 99% ^{18}O equilibration ($t_{99\%}$) can calculated using the relationship between kinetic rate constants for CO_2 hydration (see Usdowski et al., 1991) as:

$$t_{99\%} = -\ln(0.01) \cdot \tau \quad \text{(A1-b)}$$

Equation to calculate the oxygen equilibrium isotope fractionation factor between $\mathrm{HCO_3^-}$ and $\mathrm{H_2O}$ given by Mook et al. (2005):

$$^{18}\varepsilon_{HCO_3^- - H_2O} = 2.59 \pm 0.00(10^6\,\mathrm{T}^{-2}) + 1.89 \pm 0.04 \quad \text{(A2)}$$

where, T is the temperature in Kelvin.

Table A1. Full experimental description of batches 1-4 including sample ID, temperature, pH, $\delta^{13}C$, $\delta^{18}O$, and experimental notes recorded at the time of the individual experiment.

Batch #	Sample ID	T (°C)	pH	$\delta^{13}C$ (‰; VPDB)	2σ S.D.	$\delta^{18}O$ (‰; vs. VSMOW)	2σ S.D.	Experimental notes:
1	AUG21_2017TEST1	21	8.2	-30.78575	0.2503	19.59752198	0.0032	Started timer once BaCl2 solution started bubbling in reactor (~30sec delay from when solution was added). Trial run with increased BaCl2 concentration: 0.3M BaCl2 +tris solution. Spilled some sample during filtering. 16 hour equilibration period.
1	AUG22_2017TEST2	21	8.2	-30.90925	0.5374	19.5996828	0.19	Duplicate run of AUG21_2017TEST1.
1	AUG23_2017TEST3	21	8.2	-31.41544	0.1024	19.62618472	0.0224	Increased BaCl2 concentration: 0.2M BaCl2.Tubing seal on stock solution vessel came loose. Did quick fix but may cause unreliable data for this run. Bubbling delay time ~53 seconds. 16 hour equilibration period
1	AUG24_2017TEST4	21	8.2	-31.02982887	0.5499	19.8139067	0.1147	Duplicate of AUG23_2017TEST3: Increased BaCl2 concentration: 0.2M BaCl2. 12 second lag time before bubbling started. Total bubbling time=2min 9seconds.
1	AUG25_2017TEST5	21	8.2	-30.21725	0.0566	19.62499259	0.2208	Test run using 0.1M BaCl2 + tris solution. 16 hour equilibration period.
1	AUG29_2017TEST6	21	8.2	-30.0263526	0.2867	19.65198797	0.1987	Duplicate run of AUG25_2017TEST5, using 0.1M BaCl2. Used the last of the NaHCO3 for stock solution. Bubbling lag time was about 18.37 seconds.
1	AUG31_2017TEST7	21	10.3	-24.96875	1.7268	16.38495538	3.4587	Test run using 0.1M BaCl2 + high pH tris buffer (made on 7/5/17) with a pH 10.255. 1 minute 7 seconds bubbling lag time. 16 hour equilibration period.
1	SEPT5_2017TEST8	21	10.3	-26.22525	0.2065	15.46468575	0.2066	Duplicate run of AUG31_2017TEST7 with high pH tris buffer (pH 10.255). 40 seconds bubbling lag time.
1	SEPT7_2017TEST9	21	8.2	-29.26625	0.0141	19.59284388	0.0596	Test run with increased reactor solution volume to 20mL. 16 hour equilibration period.
1	SEPT14_2017TEST10	21	8.2	-27.99925	0.0679	19.71728154	0.0036	Duplicate run of SEPT7_2017TEST9 with increased reactor solution volume to 20mL, no bubbling lag time, some stock solution vapor condensed on reactor chamber walls.
1	SEPT18_2017TEST11	21	8.2	-29.0210756	0.1872	19.84331019	0.0721	Increased reactor solution volume to 30mL . Some stock solution vapor on reactor chamber walls. 16 hour equilibration period.
1	SEPT26_2017TEST12	21	8.2	-29.03675	0.0297	20.00942807	0.0448	Increased reactor solution volume to 40 mL. Stock solution vapor on inside reactor chamber. 16 hour equilibration period.
1	SEPT27_2017TEST13	21	8.2	-27.73210925	0.2748	19.96291099	0.2817	Duplicate test of SEPT26_2017TEST12. Some stock solution vapor inside reactor chamber.
1	OCT3_2017TEST14	21	8.2	-28.68875	0.0382	19.14628381	0.1447	Increased reactor solution volume to 40mL (volume increased in order to increase amount of precipitates collected), first time using liquid/vapor trap. Some stock solution vapor inside reactor chamber. Reactor solution formed smaller bubbles than normal when bubbling in reactor. 16 hour equilibration period.
1	OCT5_2017TEST15	21	8.2	-28.44875	0.0523	18.85992578	0.1184	Duplicate test of OCT3_2017TEST14 using new liquid/vapor catch set up. Reactor solution formed small bubbles when bubbling.
2	12_5_2017TEST1	21	8.0	-28.865	1.2869	17.41023355	0.452	Tris buffer pH 8 - 16 hours 21 mins equilibration period.
2	12_11_2017TEST2	21	8.0	-31.5	2.4042	17.0751878	0.3791	Duplicate run of 12_5_2017TEST1
2	12_13_2017TEST3	21	9.0	-31.17	0.5374	15.44635	0.1166	High pH tris buffer (pH 9) - 16 hours equilibration period.
2	1_9_2018Test4	21	9.0	-19.65	3.7618	14.2195671	0.0292	Duplicate run of 12_13_2017TEST3 - stopped experiment 5 mins early because stock solution was going into reactor

2	1_16_2018Test5	21	8.0	-30.22	0.0849	17.33806985	0.0437	Tris buffer pH 8 - 100 mL HCl added to stock solution - stock solution pH remained the same - 16 hours and 4 mins equilibration period
2	1_18_2018Test6	21	8.0	-30.75	0.0849	15.95665045	0.3645	Duplicate run of 1_16_2018Test5
2	2_5_2018Test7	21	8.0	-29.34	0.2263	16.8483876	0.0292	Tris buffer pH 8 - 24 hours equilibration period (8 hours per day for 3 days)
2	2_12_2018Test8	21	8.0	-30.65	0.1414	17.29683345	0.1604	Duplicate run of 2_5_2018Test7
3	April_4_2018_T1	25	8.5	-30.87	0.7538	16.90077845	0.468	Temperature set to 25C, 8.5 tris buffer pH. 16 hours equilibration period.
3	April_6_2018_T2	25	8.5	-30.43	1.9177	16.35336524	0.4972	Temperature set to 25C, 8.5 tris buffer pH.16 hours equilibration period.
3	April_12_2018_T3	30	8.5	-28.54	1.3746	17.82395835	1.006	Temperature set to 30C, 8.5 tris buffer pH. 16 hours equilibration period.
3	April_17_2018_T4	30	8.5	-27.75	0.1598	17.88735932	0.1735	Temperature set to 30C, 8.5 tris buffer pH. 16 hours equilibration period.
3	April_19_2018_T5	30	8.5	-29.91	0.8301	17.15489776	0.4257	Temperature set to 30C, 8.5 tris buffer pH. 16 hours equilibration period.
3	April_24_2018_T6	25	9.5	-22.84	0.0382	14.04721957	0.0015	Temperature set to 25C, 9.5 tris buffer pH. 16 hours equilibration period.
3	April_26_2018_T7	25	9.5	-23.54	0.1131	15.98996946	0.0525	Temperature set to 25C, 9.5 tris buffer pH. 16 hours equilibration period.
3	May_8_2018_T8	25	9.5	-30.18	0.1075	13.18898699	0.0146	Temperature set to 25C, 9.5 tris buffer pH. 16 hours equilibration period.
3	May_10_2018_T9	25	8.5	-30.84	1.5019	15.15029327	0.3076	Temperature set to 25C, 8.5 tris buffer pH. 16 hours equilibration period.
3	May_15_2018_T10	25	9.2	-30.86	0.0665	13.36888079	0.0773	Temperature set to 25C, 9.2 tris buffer pH, 0.5M NaHCO3 stock solution (1L volume). 16 hours equilibration period.
3	May_17_2018_T11	25	9.2	-31.65	0.0368	13.37712807	0.0364	Temperature set to 25C, 9.2 tris buffer pH, 0.5M NaHCO3 stock solution (1L volume). 16 hours equilibration period.
3	May_22_2018_T12	25	8.5	-28.60	0.0495	16.76469833	0.0889	0.2M BaCl2 concentration, 8.5 tris buffer pH, temperature set to 25C. 16 hours equilibration period.
3	May_30_2018_T13	25	8.5	-27.72	0.0509	17.18737143	0.1006	0.2M BaCl2 concentration, 8.5 tris buffer pH, temperature set to 25C. 16 hours equilibration period.
3	June_5_2018_T14	25	7.5	-27.81	0.0453	18.20281778	0.1152	8 hours equilibration time, 7.5 tris buffer pH, 2M NaHCO3 stock solution concetration (1L volume), temperature set to 25C
3	June_6_2018_T15	25	7.5	-27.04	0.2814	17.41050159	0.3238	7.5 tris buffer pH, 2M NaHCO3 stock solution concentration (1L volume), temperature set to 25C, 16 hours equilibration period.
3	JUNE_19_2018_T16	25	7.5	-29.47	0.4455	17.6126218	0.3499	7.5 tris buffer pH, 2M NaHCO3 stock solution concentration (1L volume), temperature set to 25C but water bath cooled to 10C, carried out experiment despite temperature change. 16 hours equilibration period.
3	JUNE_26_2018_T17	25	7.5	-23.85	0.4709	17.736331	0.6911	7.5 tris buffer pH, 2M NaHCO3 stock solution concentration (1L volume), temperature set to 25C. 16 hours equilibration period.
3	JUNE_28_2018_T18	25	7.5	-27.78	0.3068	18.5867699	0.1868	7.5 tris buffer pH, 2M NaHCO3 stock solution concentration (1L volume), temperature set to 25C. 16 hours equilibration period.
3	JULY_2_2018_T19	25	8.5	-23.07	0.4681	16.55439269	0.3893	8.5 tris buffer pH, 1M NaHCO3, temperature set to 25C. 16 hours equilibration period.
3	JULY_8_2018_T20	25	8.5	-23.71	0.4285	15.04410954	0.0685	8.5 tris buffer pH, 1M NaHCO3, temperature set to 25C. 16 hours equilibration period.
3	JULY_10_2018_T21	25	9.0	-23.03	0.1216	15.67399555	0.121	9.0 tris buffer pH, 1M stock solution concentration (1L volume), temperature set to 25C. 16 hours equilibration period.
3	JULY_12_2018_T22	25	9.0	-31.33	0.0057	13.19723427	0.2858	9.0 tris buffer pH, 1M stock solution concentration (1L volume), temperature set to 25C. 16 hours equilibration period.
4	JUL31_1A_2018	18	8.0	-30.51	0.1409	17.03177992	0.0117	Temperature of waterbath and stock solution=15C, actual temperature during reaction = 18°C, 21 hours equilibration time. pH 8, 1M NaHCO3 stock solution concentration. Started using syringe seal method (no stopping pump

								when inputting reactor solution to maintain closed system) - used pump test to assure no leaks
4	AUG5_1B_2018	18	8.0	-31.78	0.2011	17.4268655	0.2006	Dulicate run of JUL31_1A_2018
4	AUG14_2A_2018	25	8.0	-29.95	0.0474	20.13714341	0.1642	T=25C, using 0.4M HEPES buffer with pH 8.0, 16 hours equilibration time
4	AUG20_2B_2018	25	8.0	-27.75	0.0161	18.75373723	0.147	Duplicate run of AUG14_2A_2018
4	OCT11_3A_2018	25	8.0	-29.76	1.1063	17.24090965	0.0427	The first out of 4 runs under the following conditions: pH 8, T=25C, 16 hours equilibration time, tris buffer.
4	OCT17_3B_2018	25	8.0	-29.03	0.0512	18.76019501	0.1222	Duplicate 2 out of 4
4	OCT19_3C_2018	25	8.0	-29.09	0.0804	18.81784988	0.0026	Duplicate 3 out of 4
4	OCT23_3D_2018	25	8.0	-30.29	0.0311	17.98842639	0.1655	Duplicate 4 out of 4
4	OCT25_4A_2018	25	8.0	-32.22	0.2232	20.07582386	0.2128	pH 8, T=25C, using HEPES buffer - possible air leak from bad seal on a tube
4	OCT30_4B_2018	25	8.0	-29.86	0.0302	19.07163178	0.0774	Duplicate run of OCT25_4A_2018
4	NOV7_5A_2018	25	8.0	-29.39	0.161	18.46816709	0.144	pH 8, T=25C, 16 hour equilibration period, tris buffer.
4	NOV14_5B_2018	25	8.0	-29.80	0.4068	19.39879897	0.0728	Duplicate run of NOV7_5A_2018

Table A2. Initial mass of Ba measured from $BaCl_2 \bullet 2H_2O$ crystals and final mass of precipitated $BaCO_3$ sample for all for batches. Moles of Ba were calculated from both the initial mass of Ba and final mass of Ba then subtracted to yield the remaining moles of Ba in solution.

Batch #	Sample Name	Initial Mass Ba (g)	Initial (moles Ba)	$BaCO_3$ Sample Weight (g)	Final (Moles Ba from $BaCO_3$)	Initial - Final (moles Ba)
1	AUG21_2017TEST1	0.7317	0.005328	0.008400	0.000061	0.005267
1	AUG22_2017TEST2	0.7396	0.005386	0.014800	0.000108	0.005278
1	AUG23_2017TEST3	0.4900	0.003568	0.008500	0.000062	0.003506
1	AUG24_2017TEST4	0.4901	0.003569	0.009500	0.000069	0.003500
1	AUG25_2017TEST5	0.2488	0.001812	0.005100	0.000037	0.001775
1	AUG29_2017TEST6	0.2577	0.001877	0.006300	0.000046	0.001831
1	AUG31_2017TEST7	0.2542	0.001851	0.040900	0.000298	0.001553
1	SEPT5_2017TEST8	0.2541	0.001850	0.082800	0.000603	0.001247
1	SEPT7_2017TEST9	0.4923	0.003585	0.045700	0.000333	0.003252
1	SEPT14_2017TEST11	0.4757	0.003464	0.064300	0.000468	0.002996
1	SEPT18_2017TEST12	0.7353	0.005354	0.075900	0.000553	0.004802
1	SEPT26_2017TEST14	0.9518	0.006931	0.149700	0.001090	0.005841
1	SEPT27_2017TEST15	0.9526	0.006937	0.175500	0.001278	0.005659
1	OCT3_2017TEST16	0.9513	0.006927	0.087900	0.000640	0.006287
1	OCT5_2017TEST17	0.9517	0.006930	0.044200	0.000322	0.006608
Averages	**[g] or [moles]**	0.5985	0.004358	0.054633	0.000398	0.003960

Batch #	Sample Name	Initial Mass Ba (g)	Initial (moles Ba)	$BaCO_3$ Sample Weight (g)	Final (Moles Ba from $BaCO_3$)	Initial - Final (moles Ba)
2	12_5_TEST1	0.5048	0.003676	n/a	n/a	n/a
2	12_11_TEST2	0.4975	0.003623	0.037309	0.000272	0.003351
2	12_13_TEST3	0.4803	0.003497	0.019230	0.000140	0.003357
2	1_9_Test4	0.4682	0.003409	0.125090	0.000911	0.002498
2	1_16_Test5	0.4883	0.003556	0.048749	0.000355	0.003201
2	1_18_Test6	0.4917	0.003580	0.002519	0.000018	0.003562
2	2_5_Test7	0.4908	0.003574	0.062690	0.000456	0.003117
2	2_12_Test8	0.4900	0.003568	0.112010	0.000816	0.002752
Averages	**[g] or [moles]**	0.4867	0.003544	0.058228	0.000424	0.003120

Batch #	Sample Name	Initial Mass Ba (g)	Initial (moles Ba)	$BaCO_3$ Sample Weight (g)	Final (Moles Ba from $BaCO_3$)	Initial - Final (moles Ba)
3	April_4_T1	0.4951	0.003605	0.053399	0.000389	0.003216
3	April_6_T2 (T1 duplicate)	0.4910	0.003575	0.111730	0.000814	0.002762
3	April_12_T3	0.4947	0.003602	0.039770	0.000290	0.003313
3	April_17_T4 (T3 duplicate)	0.4812	0.003504	0.028480	0.000207	0.003297
3	April_19_T5 (T3 duplicate)	0.4909	0.003575	0.054200	0.000395	0.003180
3	April_24_T6	0.4939	0.003596	0.053729	0.000391	0.003205
3	April_26_T7 (T6 duplicate)	0.4851	0.003532	0.137450	0.001001	0.002531
3	May_8_T8 (T6 duplicate)	0.4848	0.003530	0.023720	0.000173	0.003357
3	May_10_T9	0.4986	0.003631	0.025549	0.000186	0.003445
3	May_15_T10	0.4982	0.003628	0.092319	0.000672	0.002956
3	May_17_T11 (T10 duplicate)	0.4856	0.003536	0.026589	0.000194	0.003342
3	May_22_T12	0.9894	0.007205	0.008669	0.000063	0.007141
3	May_30_T13 (T12 duplicate)	0.9797	0.007134	0.023339	0.000170	0.006964
3	June_5_T14	0.4891	0.003561	0.136720	0.000996	0.002566
3	June_6_T15	0.4856	0.003536	0.046750	0.000340	0.003196
3	JUNE_19_T16	0.4996	0.003638	0.021369	0.000156	0.003482
3	JUNE_26_T17	0.4974	0.003622	0.061670	0.000449	0.003173
3	JUNE_28_T18 (T17 duplicate)	0.4945	0.003601	0.090880	0.000662	0.002939
3	JULY_2_T19	0.4875	0.003550	0.170060	0.001238	0.002312
3	JULY_8_T20 (T19 duplicate)	0.4886	0.003558	0.089730	0.000653	0.002904
3	JULY_10_T21	0.4967	0.003617	0.051580	0.000376	0.003241
3	JULY_12_T22 (T21 duplicate)	0.4961	0.003612	0.063149	0.000460	0.003153
Averages	**[g] or [moles]**	0.5365	0.003907	0.064130	0.000467	0.003440

Batch #	Sample Name	Initial Mass Ba (g)	Initial (moles Ba)	$BaCO_3$ Sample Weight (g)	Final (Moles Ba from $BaCO_3$)	Initial - Final (moles Ba)
4	JUL31_1A_2018	0.4854	0.003535	0.043399	0.000316	0.003219
4	AUG5_1B_2018	0.4806	0.003500	0.041173	0.000300	0.003200
4	AUG14_2A_2018	0.4890	0.003561	0.038770	0.000282	0.003278
4	AUG20_2B_2018	0.4899	0.003567	0.038480	0.000280	0.003287
4	OCT11_3A_2018	0.4988	0.003632	0.058995	0.000430	0.003203
4	OCT17_3B_2018	0.4920	0.003583	0.048373	0.000352	0.003230
4	OCT19_3C_2018	0.4933	0.003592	0.053845	0.000392	0.003200
4	OCT23_3D_2018	0.4891	0.003561	0.043614	0.000318	0.003244
4	OCT25_4A_2018	0.4906	0.003572	0.046548	0.000339	0.003233
4	OCT30_4B_2018	0.5091	0.003707	0.053429	0.000389	0.003318
4	NOV7_5A_2018	0.4909	0.003575	0.048587	0.000354	0.003221
4	NOV14_5B_2018	0.4947	0.003602	0.046874	0.000341	0.003261
Averages	**[g] or [moles]**	0.4920	0.0036	0.0468	0.0003	0.0032

Table A3. Average ^{13}KIFs and ^{18}KIFs during CO_2 hydration for batches 1-4. KIFs are organized by temperature and pH. The value of n represents the amount of samples used to calculate the average KIFs at various parameters specified for each batch.

Batch #	n	Temperature (°C)	pH	$^{13}KIF_{CO_2(g)-BaCO_3}$ (‰)	$^{18}KIF_{HCO_3^-(instant)-BaCO_3}$ (‰)	$^{18}KIF_{CO_2(g)-BaCO_3}$ (‰)
1	13	21	8.2	19.01527401	5.066384439	18.74043201
1	2	21	10.3	14.84607724	8.721872782	22.44565371
2	6	21	8.0	19.68518172	7.667084107	21.37651451
2	2	21	9.0	14.68712074	9.806589383	23.54512801
3	5	25	7.5	16.51054333	6.229833716	19.66472916
3	3	30	8.5	19.16149551	5.878301548	18.99899103
3	7	25	8.5	17.25114666	7.844652521	21.30110857
3	2	25	9.0	16.5145848	9.677238988	23.15816321
3	2	25	9.2	20.77503467	10.73446243	24.2295024
3	3	25	9.5	14.77486575	9.7038391	23.18511848
4	2	18	8.0	20.30823905	7.049878372	21.73789001
4	10	25	8.0	19.6152262	5.280787852	18.87114422

REFERENCES

Adkins J. F., Boyle E. A., Curry W. B. and Lutringer A. (2003) Stable isotopes in deep-sea corals and a new mechanism for "vital effects." *Geochim. Cosmochim. Acta* **67**, 1129–1143.

Affek H. P. and Eiler J. M. (2006) Abundance of mass 47 CO_2 in urban air, car exhaust, and human breath. *Geochim. Cosmochim. Acta* **70**, 1–12.

ANSI/ASHRAE Standard. (2016) *Ventilation for Acceptible Indoor Air Quality (ANSI Approved)*, ASHRAE, Atlanta, GA.

Beck W. C., Grossman E. L. and Morse J. W. (2005) Experimental studies of oxygen isotope fractionation in the carbonic acid system at 15°, 25°, and 40°C. *Geochim. Cosmochim. Acta* **69**, 3493–3503.

Bigeleisen J. (1965) Chemistry of Isotopes: Isotope chemistry has opened new areas of chemical physics, geochemistry, and molecular biology. *Science (80).* **147**, 463–471.

Bigeleisen J. and Wolfsberg M. (1958) *Theoretical and experimental aspects of isotope effects in chemical kinetics*. 1st ed., Adv. Chem. Phys.

Böttcher M. E. (1996) $^{18}O/^{16}O$ and $^{13}C/^{12}C$ fractionation during the reaction of carbonates with phosphoric acid effects of cationic substitution and reaction temperature. *Isotopes Environ. Health Stud.* **32**, 299–305.

Brenninkmeijer C. A. M., Kraft P. and Mook W. G. (1983) Oxygen isotope fractionation between CO_2 and H_2O. *Chem. Geol.* **41**, 181–190.

Brown J. G. E., Bird D. K., Kendelewicz T., Maher K., Mao W., Johnson N., Rosenbauer R. J. and García Del Real P. (2009) Geological Sequestration of CO_2 : Mechanisms and Kinetics of CO_2 Reactions in Mafic and Ultramafic Rock Formations. *2009 Annu. Rep. to Glob. Clim. Energy Proj.* **c**, 1–27.

Caldeira K. and Wickett M. E. (2003) Anthropogenic carbon and ocean pH, *Nature*. 1–7.

Clark I. D., Fontes J. C. and Fritz P. (1992) Stable isotope disequlibria in travertine from high pH waters: Laboratory investigations and field observations from Oman. *Geochim. Cosmochim. Acta* **56**, 2041–2050.

Clark I. D. and Lauriol B. (1992) Kinetic enrichment of stable isotopes in cryogenic calcites. *Chem. Geol.* **102**, 217–228.

Coplen T. B., Winograd I. J., Landwehr J. M., Riggs A. C. (1994) 500,000-year stable carbon isotopic record from Devils Hole, Nevada. *American Association for the Advancement of Science* **263**(5145), 361-365.

Coplen T. B., Kendall C., and Hopple J. (1983) Comparison of stable isotope reference samples. *Nature* **302**, 236-238.

Daëron M., Drysdale R. N., Peral M., Huyghe D., Blamart D., Coplen T. B., Lartaud F. and Zanchetta G. (2019) Most Earth-surface calcites precipitate out of isotopic equilibrium. *Nat. Commun.* **10**, 429.

Deines P., Langmuir D., and Harmon R. S. (1974) Stable carbon isotope ratios and the existence of a gas phase in the evolution of carbonate ground waters. *Geochim. Cosmochim. Acta* **38**, 1147-1164.

Dunsmore H. E. (1992) A geological perspective on global warming and the possibility of carbon dioxide removal as calcium carbonate mineral. *Energy Conserv. Manag.* **33**, 565–572.

Eigen M., Kustin K. and Maass G. (1961) Die geschwindigkeit der hydration von SO_2 in wabriger losung. *Z. Phys. Chem.* **30**, 130–136.

Emrich K., Ehhalt D. H., and Vogel J.C. (1970) Carbon isotope fractionation during the precipitation of calcium carbonate. *Earth Planet. Sci.* **8**, 363-371.

Guo W. (2008) Carbonate clumped isotope thermometry: application to carbonaceous chondrites and effects of kinetic fractionation. California Institute of Technology.

Guo W. and Zhou C. (2019) Triple oxygen isotope fractionation in the DIC-H_2O-CO_2 system: A numerical framework and its implications. *Geochim. Cosmochim. Acta* **246**, 541–564.

Hayes J. M. (2001) actionation Hydr dro Fractionation of the Isotopes of Carbon and Hydrogen Processes * in Biosynthetic Pr ocesses. *Rev. Mineral. Geochemistry* **43**, 225–277.

Hayes J. M. (2002) *Practice and principles of isotopic measurements in oranic geochemistry.*, Woods Hole.

Hopkinson B. M., Dupont C. L., Allen A. E. and Morel F. M. M. (2011) Efficiency of the CO_2-concentrating mechanism of diatoms. *Proc. Natl. Acad. Sci.* **108**, 3830–3837.

Inoue H. and Sugimura Y. (1985) Carbon isotopic fractionation during the CO_2 exchange process between air and sea water under equilibrium and kinetic conditions. *Geochim. Cosmochim. Acta* **49**, 2453–2460.

Johnson K. S. (1982) Carbon dioxide hydration and dehydration in sea water. *Limnol. Ocean.* **27**, 849–855.

Kern D. M. (1960) The hydration of carbon dioxide. *J. Chem. Educ.* **37**, 14.

Kim S.T. and O'Neil J.R. (1997) Equilibrium and nonequilibrium oxygen isotope effects in

synthetic carbonates. *Geochemica et Cosmochimica Acta*. **61**(16), 3461-3475.

Lacella D., Lauriol B. and Clark I. D. (2009) Formation of seasonal ice bodies and associated cryogenic carbonates in Caverne De L'ours, Quebec, Canada: Kinetic isotope effects and Pseudo-biogenic crystal structures. *J. Cave Karst Stud.* **71**, 49–62.

Marlier J. F. and O'Leary M. H. (1984) Carbon Kinetic Isotope Effects on the Hydration of Carbon Dioxide and the Dehydration of Bicarbonate Ion. *J. Am. Chem. Soc.* **106**, 5054–5057.

McConnaughey T. (1989) ^{13}C and ^{18}O isotopic disequilibrium in biological carbonates: II. In vitro simulation of kinetic isotope effects. *Geochim. Cosmochim. Acta* **53**, 163–171.

McConnaughey T. A. (2003) Sub-equilibrium oxygen-18 and carbon-13 levels in biological carbonates: Carbonate and kinetic models. *Coral Reefs* **22**, 316–327.

McKinney C. R., McCrea J. M., Epstein S., Allen H. A. and Urey H. C. (1950) Improvements in mass spectrometers for the measurement of small differences in isotope abundance ratios. *Rev. Sci. Instrum.* **21**, 724–730.

Mickler P. J., Banner J. L., Stern L., Asmerom Y., Edwards R. L. and Ito E. (2004) Stable isotope variations in modern tropical speleothems: Evaluating equilibrium vs. kinetic isotope effects. *Geochim. Cosmochim. Acta* **68**, 4381–4393.

Mickler P. J., Stern L. A. and Banner J. L. (2006) Large kinetic isotope effects in modern speleothems. *Bull. Geol. Soc. Am.* **118**, 65–81.

Mook W. G. (1986) ^{13}C in atmospheric CO_2. *Netherlands J. Sea Res.* **20**, 211–223.

Nguyen Minh Tho, Matus M. H., Jackson V. E., Ngan V. T., Rostad J. R. and Dixon D. A. (2008) Mechanism of the hydration of carbon dioxide: Direct participation of H_2O versus microsolvation. *J. Phys. Chem. A* **112**, 10386–10398.

Nguyen M. T., Matus M. H., Jackson V. E., Ngan V. T., Rustad J. R. and Dixon D. A. (2008) No Mechanism of the hydration of carbon dioxide: Direct participation of H_2O verses microsolvation. *J. Phys. Chem.* **112**, 10386–10398.

Dr. Pieter Tans, NOAA/ESRL(www.esrl.noaa.gov/gmd/ccgg/trends/) and Dr. Ralph Keeling, Scripps Institute of Oceanography(Scrippsco2.ucsd.edu/), 2019.

O'Leary M. H., Madhaven S. and Paneth P. (1992) Physical and chemical basis of carbon isotope fractionation in plants. *Plant Cell Environ.* **15**, 1099–1104.

Sade Z. and Halevy I. (2018) Corrigendum to "New constraints on kinetic isotope effects during CO2(aq) hydration and hydroxylation: Revisiting theoretical and experimental data".

Geochim. Cosmochim. Acta **225**, 237-240.

Sade Z. and Halevy I. (2017) New constraints on kinetic isotope effects during $CO_{2(aq)}$ hydration and hydroxylation: Revisiting theoretical and experimental data. *Geochim. Cosmochim. Acta* **214**, 246–265.

Scholl M. A., Giambelluca T. W., Gingerich S. B., Nullet M. A., and Loope L. L. (2007) Cloud water in windward and leeward mountain forests: The stable isotope signature of orographic cloud water. *Water Resources Research*. **43**, W12411.

Sharp Z. D. (2007) *Principles of stable isotope geochemistry*. 2nd ed., Pearson/Prentice Hall.

Siegenthaler U. and Münnich K. O. (1981) $^{12}C/^{13}C$ fractionation during CO_2 transfer from air to sea. *Carbon Cycle Model.*, 249–251.

Stirling A. (2011) HCO_3^- formation from CO_2 at High pH: Ab initio molecular dynamics study. *J. Phys. Chem.* **115**, 14683–14687.

Stirling A. and Papai I. (2010) H_2CO_3 Forms via HCO_3^- in Water. *J. Phys. Chem. B* **114**, 16854–16859.

Swart P. K. (1983) Carbon and oxygen isotope fractionation in scleractinian corals: a review. *Earth-Science Rev.* **19**, 51–80.

Szaran J. (1998) Carbon isotope fractionation between dissolved and gaseous carbon dioxide. *Chem. Geol.* **150**.

Tautermann C. S., Voegele A. F., Loerting T., Kohl I., Hallbrucker A., Mayer E. and Liedl K. R. (2002) Towards the experimental decomposition rate of carbonic acid (H_2CO_3) in aqueous solution. *Chem. - A Eur. J.* **8**, 66–73.

Tresguerres M. and Hamilton T. J. (2017) Acid–base physiology, neurobiology and behaviour in relation to CO_2 -induced ocean acidification . *J. Exp. Biol.* **220**, 2136–2148.

Tripati A. K., Hill P. S., Eagle R. A., Mosenfelder J. L., Tang J., Schauble E. A., Eiler J. M., Zeebe R. E., Uchikawa J., Coplen T. B., Ries J. B. and Henry D. (2015) Beyond temperature: Clumped isotope signatures in dissolved inorganic carbon species and the influence of solution chemistry on carbonate mineral composition. *Geochim. Cosmochim. Acta* **166**, 344–371.

Uchikawa J. and Zeebe R. E. (2012) The effect of carbonic anhydrase on the kinetics and equilibrium of the oxygen isotope exchange in the CO_2-H_2O system: Implications for $\delta^{18}O$ vital effects in biogenic carbonates. *Geochim. Cosmochim. Acta* **95**, 15–34.

Urey H. C. (1948) Oxygen isotopes in nature and in the laboratory. *Science (80-.).* **108**, 489–496.

Usdowski E., Michaelis J., Bottcher M. E., and Hoefs J. (1991) Factors for the oxygen isotope equilibrium fractionation between aqueous and gaseous CO_2, carbonic acid, bicarbonate, carbonate, and water (19°C). *Z. Phys. Chem.* **170**, 237-249.

Usdowski E. and Hoefs J. (1990) Kinetic $^{13}C/^{12}C$ and $^{18}O/^{16}O$ effects upon dissolution and outgassing of CO_2 in the system CO_2-H_2O. *Chem. Geol. (Isotope Geosci. Sect.* **80**, 109–118.

Vogel J. C., Grootes P. M. and Mook W. G. (1970) Isotopic fractionation between gaseous and dissolved carbon dioxide. *Zeitschrift für Phys.* **230**, 225–238.

Wang B. and Cao Z. (2013) How water molecules modulate the hydration of CO_2 in water solution: Insight from the cluster-continuum model calculations. *J. Comput. Chem.* **34**, 372–378.

Wanninkof R. (1985) Kinetic fractionation of the carbon isotopes ^{13}C and ^{12}C during transfer of CO_2 from air to seawater. *Tellus B* **37 B**, 128–135.

Watkins J. M., Nielsen L. C., Ryerson F. J. and DePaolo D. J. (2013) The influence of kinetics on the oxygen isotope composition of calcium carbonate. *Earth Planet. Sci. Lett.* **375**, 349–360.

Zeebe R. (2014) Kinetic fractionation of carbon and oxygen isotopes during hydration of carbon dioxide. *Geochim. Cosmochim. Acta* **139**, 540–552.

Zeebe R. E. (1999) An explanation of the effect of seawater carbonate concentration on foraminiferal oxygen isotopes. *Geochim. Cosmochim. Acta* **63**, 2001–2007.

Zeebe R. E. and Wolf-Gladrow D. (2001) *CO_2 in seawater: equilibrium, kinetics, isotopes*., Elsevier Science Publishers B.V., Amsterdam.

Zhang J., Quay P. D. and Wilbur D. O. (1995) Carbon isotope fractionation during gas-water exchange and dissolution of CO_2. *Geochim. Cosmochim. Acta* **59**, 107–114.